

A11102 977847

REFERENCE

NIST
PUBLICATIONS

NBSIR 87-3075

NATL INST OF STANDARDS & TECH R.I.C.



A11102977847

Read, D. T./Postweld heat treatment crite
QC100 . U56 NO.87-3075 1988 V19 C.1 NBS-P

WELD HEAT TREATMENT IA FOR REPAIR WELDS IN 2-1/4Cr-1Mo SUPERHEATER HEADERS AN EXPERIMENTAL STUDY

D. T. Read
H. I. McHenry

National Bureau of Standards
U.S. Department of Commerce
Boulder, Colorado 80303-3328

August 1988



g America's Progress
1913-1988

QC
100
.U56
#87-3075
1988

NATIONAL INSTITUTE OF STANDARDS &
TECHNOLOGY
Research Information Center
Gaithersburg, MD 20899

NBSIR 87-3075

NBSR
QC100
USG
NO. 87-3075
1988

POSTWELD HEAT TREATMENT CRITERIA FOR REPAIR WELDS IN 2-1/4Cr-1Mo SUPERHEATER HEADERS

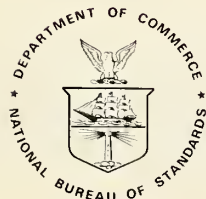
AN EXPERIMENTAL STUDY

D. T. Read
H. I. McHenry

Fracture and Deformation Division
Institute for Materials Science and Engineering
National Bureau of Standards
Boulder, Colorado 80303-3328

August 1988

Supported in part by
Naval Sea Systems Command
Washington, DC 20362-5101



U.S. DEPARTMENT OF COMMERCE, C. William Verity, Secretary

NATIONAL BUREAU OF STANDARDS, Ernest Ambler, Director

IMPORTANT NOTICE

Identification of commercial bibliographic services by trade name does not imply recommendation or endorsement by the National Bureau of Standards, nor does it imply that the specific services identified are the best available.

CONTENTS

ABSTRACT	v
1. STATEMENT OF THE PROBLEM: DOES POSTWELD HEAT TREATMENT OF REPAIR WELDS IN SUPERHEATER HEADERS CONTRIBUTE TO THE PREVENTION OF FRACTURE?	1
1.1 Literature Review	2
2. APPROACH: ELASTIC-PLASTIC FRACTURE MECHANICS	3
3. WELD METAL: 2½Cr-1Mo	4
4. EXPERIMENTAL SPECIFICS: WELD AND SPECIMEN GEOMETRIES AND TEST PROCEDURES	5
4.1 Wide Plates	7
4.2 Standard Specimens	8
5. EXPERIMENTAL RESULTS	9
5.1 Weldment Characterization	9
5.2 Wide-Plate Results	10
5.3 J-Integral Fracture-Toughness Tests	14
5.4 Tensile Tests	16
6. RESULTS AND DISCUSSION: DIRECT MEASUREMENT OF THE J-INTEGRAL IN THE WIDE PLATE	17
7. IMPLICATIONS	21
8. NOTE ON THE EXPERIMENTAL APPROACH	22
9. ACKNOWLEDGMENTS	22
10. REFERENCES	23
APPENDIX A. DESCRIPTION OF THE WELDING PROCEDURE	25
APPENDIX B. ULTRASONIC MEASUREMENTS OF RESIDUAL STRESS	27
APPENDIX C. MECHANICAL MEASUREMENTS OF RESIDUAL STRESS	29
APPENDIX D. MEASUREMENT OF APPLIED J-INTEGRAL PRODUCED BY RESIDUAL STRESS	37

ABSTRACT

Wide-plate and standard-size specimens cut from repair welds in 2½Cr-1Mo plate were tested as-welded and after postweld heat treatment (PWHT). Wide plates were prepared with surface cracks and tube-hole-ligament cracks in simulated repair welds made with the shielded-metal-arc process. The plates were instrumented with strain and displacement gages for direct measurement of the applied J-integral. After notching and fatigue precracking, the plates were tested in bending. Pop-ins occurred in the as-welded plates, but not in the PWHT plates.

Three-point-bend specimens with cracks oriented in the TS direction were used to measure weld-metal and heat-affected-zone (HAZ) toughness values. Results of direct measurements of the applied J-integral on the wide plates were compared with critical J-value measurements of three-point-bend specimens. The comparison indicated that PWHT was highly beneficial, because it reduced the crack-driving force from residual stresses and increased the weld-metal and HAZ toughness. In the as-welded condition, very low toughness values were measured at the HAZ. These low toughness values, together with the measured crack-driving forces, indicated critical crack depths of a few millimeters.

To extend the usefulness of these results, a new approach to the problem of the applied J-integral produced by residual stresses is being explored: strain-gage measurements made during notching are analyzed to obtain an applied J-integral as a function of crack depth. The preliminary results are encouraging. The residual-stress-produced J-value is roughly equivalent to that produced by a remote elastic loading to the same stress level.

Key words: Fracture; hydrotest; J-integral; pressure vessel; residual stress; safety; stress relief.

POSTWELD HEAT TREATMENT CRITERIA FOR REPAIR WELDS
IN 2½Cr-1Mo SUPERHEATER HEADERS

AN EXPERIMENTAL STUDY

1. STATEMENT OF THE PROBLEM: DOES POSTWELD HEAT TREATMENT OF REPAIR WELDS
IN SUPERHEATER HEADERS CONTRIBUTE TO THE PREVENTION OF FRACTURE?

Postweld heat treatment (PWHT) of repair welds made in superheater headers is currently mandated by documents, including MIL-STD-278E(SH) [1]. Omission of the PWHT is allowed in certain circumstances listed in the standard; these include several classes of welds in grooves 6 mm (1/4 in) deep or less. The standard indicates that NAVSEA may specifically approve omission of the PWHT in "other welds."

The PWHT of repair welds can entail logistical problems above and beyond the consumption of time and energy. Specialized equipment and extensive setup procedures may be needed because the superheater headers are located deep within the hull. There are no known reports of fractures or failures caused by omission of the PWHT in the allowed circumstances. Specific justification for the original inclusion of the PWHT requirement in the MIL-STD is unavailable. The purpose of the PWHT requirement is now assumed to be fracture prevention in the boiler components.

Fracture of boiler components is unacceptable because of danger to personnel, loss of ship function, and cost of repair. The actual benefits of PWHT should be carefully evaluated so that they can be balanced against the associated costs.

Risks of superheater header fracture occur during hydrostatic testing (at room temperature) and during operation (at superheated steam temperature). The three causes of fracture are high stresses, brittle material, and large defects. The stresses are highest and the material is most

brittle during hydrotest. Inspection and maintenance procedures are intended to eliminate large defects before hydrotest; however, the boilers have many welds that can contain undetected and potentially dangerous cracks.

This program addresses fracture at weld cracks during a hydrotest after weld repair. It seeks to identify the difference in fracture safety between a weld-repaired component that is given a PWHT and a component that receives no PWHT. The technical information obtained in this program will support Navy administrative decisions on stress relief-criteria for repair welds.

1.1 Literature Review

Two approaches were adopted to take advantage of previous research on postweld treatment of repair welds in 2½Cr-1Mo steel pressure vessels: computerized searches of abstracts on file with abstract services, and tracking of significant references starting with recent high-quality work. The computer index searches were not productive; however, several useful references were found by reference tracking.

The key word combination (weld fracture .and. (pressure vessel .or. stress relief)) was sought in abstracts in Compendex (which contains engineering information). Two hundred and forty-one resulting abstracts were examined. The combination (weld .and. stress relief .and. pressure vessel) was sought in the Weldasearch file. Ninety-eight resulting abstracts were examined. These efforts confirmed the lack of a good data base on stress relief of repair welds in pressure vessels. The most useful references (tracked manually) are listed below.

An excellent review of the metallurgy of 2½Cr-1Mo was given by C. D. Lundin, B. J. Kruse, and M. R. Pendley [2]. The effects of PWHT time and temperature on the toughness and tensile properties of a multipass submerged arc weld in 2½Cr-1Mo were reported by R. A. Swift and H. C. Rogers [3]. This report confirmed the large differences between as-welded (AW) and PWHT weld metal found in the present study.

The first report, and still one of the most accessible and unambiguous reports, of the effect of residual stress on the fracture of wide plates was given by T. W. Greene [4]. It provides the precedent for the use of wide plates in bending in the present study. Unfortunately, this study was conducted well before fracture mechanics reached its current state of development.

The effect of PWHT on 2½Cr-1Mo base-metal Charpy-impact toughness was reported by J. P. Gudas, C. A. Zanis, E. J. Czyryca, G. L. Franke, E. M. Hackett, and W. A. Palko [5]. In their study, ductile tearing occurred at room temperature in 2½Cr-1Mo base metal, a behavior not observed in the present study, possibly because a different specimen orientation was used.

A recent literature review of the weldability and properties of 2½Cr-1Mo steel by J. M. Blackburn [6] concentrates on the controllable aspects of the welding process, especially preheat, and their effects on the weld metallurgy.

2. APPROACH: ELASTIC-PLASTIC FRACTURE MECHANICS

Fracture mechanics is the branch of engineering science that seeks to measure the resistance of materials to fracture and to balance applied stresses, material resistance to fracture, and defect size, so that the risk of fracture in service is appropriately controlled. The present approach centers on a fracture mechanics evaluation of severe artificial defects in simulated repair welds in large, thick plates of superheater header material, 2½Cr-1Mo steel. Large plates are needed to retain the residual stresses and to simulate the actual structural behavior. Plates with PWHT are compared with AW plates. Room-temperature tests conveniently match the hydrotest temperature.

Included in the approach are evaluations of the residual stress present in the PWHT and AW plates and conventional small-specimen tests of weld

metal in both PWHT and AW conditions. The small-specimen tests include weld-metal fracture-toughness, Charpy-impact-toughness, and tensile-property tests, as well as metallographic examination.

Analysis and interpretation of the test data will contribute to the development of guidelines for stress relief of boiler components following weld repair.

3. WELD METAL: 2½Cr-1Mo

Steel plate manufactured to ASTM Standard A387 Grade 22 Class 1 (1984), in the annealed condition, was obtained from a commercial source in the form of two plates, each 5 cm (2 in) thick by 2 m (80 in) by 3.7 m (144 in). The plate chemistry supplied by the manufacturer is given in table 1, along with a check analysis performed by a commercial laboratory.

The welding electrodes used were the same type, E9018-B3L, and from the same manufacturer as those used by the Navy [1]. In the electrode designation, L indicates low carbon, which is now standard. A preheat of 200°C (400°F) was used. The welding procedures are detailed in Appendix A of this report, and the chemical compositions of the weld and base metal are given in table 1. The differences between the AW and PWHT specimens are thought to reflect the level of accuracy in the analysis rather than actual differences caused by PWHT.

According to [1], the holding temperature for PWHT of 2½Cr-1Mo vessels should be between 730 and 775 °C (1350 to 1425 °F). The holding time should be 1 hour per 2.5 cm of thickness (1 hour per inch of thickness). Following [5], the PWHT was performed as follows:

- a. Heat from 200 to 745 °C (400 to 1375 °F) at a rate less than 110 °C (200 °F) per hour;
- b. Hold at 745 °C (1375 °F) for 2 hours;
- c. Cool to 200 °C (400 °F) at a rate less than 110 °C (200 °F) per hour;
- d. Air cool.

Table 1. Chemical compositions of materials, in mass percent.

Element	Base Metal		Weld	
	Mfr.	Check	AW	PWHT
Cr	2.24	2.14	2.43	2.41
Mo	0.98	0.86	1.05	1.02
C	0.11	0.097	0.042	0.035
Mn	0.47	0.45	0.76	0.70
Ni	NA	0.14	0.05	0.05
P	0.009	0.010	0.024	0.024
S	0.015	0.012	0.018	0.016
Si	0.20	0.18	0.048	0.043
Al	NA	0.011	0.012	0.010
Ti	NA	0.002	0.007	0.006
Co	NA	0.011	0.017	0.016
V	NA	0.008	0.010	0.009
Cu	NA	0.083	0.056	0.054
Fe	bal.	bal.	bal.	bal.

4. EXPERIMENTAL SPECIFICS:

WELD AND SPECIMEN GEOMETRIES AND TEST PROCEDURES

The test matrix, including wide-plate and small-specimen tests of repair welds AW and after PWHT, is illustrated in figure 1. Two types of repair welds were used: trough welds and simulated tube-hole-ligament repairs.

The Welding Group at David Taylor Naval Ship Research and Development Center (DTNSRDC), Annapolis, has developed a standard repair-weld test geometry consisting of a trough in a plate with specified dimensions (fig. 2). The trough is 20 cm (8 in) long by 4 cm (1-1/2 in) deep in a plate that is 5 cm (2 in) thick, 45 cm (18 in) long, and 30 cm (12 in) wide. The geometries of six of the eight troughs welded in this study were based on the DTNSRDC geometry—two for wide-plate tests and four for standard-specimen tests (fig. 1). The other two were designed to simulate a repair to a ligament between tube holes (discussed below); see figure 3.

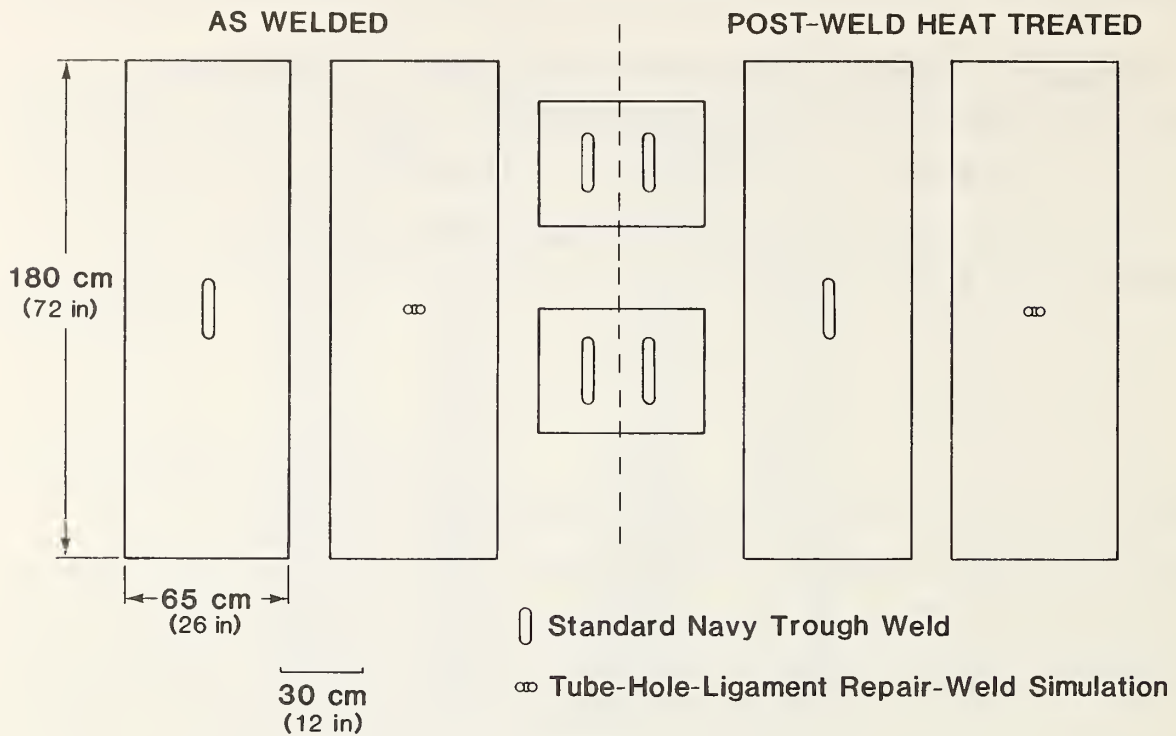


Figure 1. Weld and plate geometries used to test benefits of PWHT in 2½Cr-1Mo repair welds. Summary of simulated A387, Grade 22, Class 1 (E9018-B3L) repair welds.

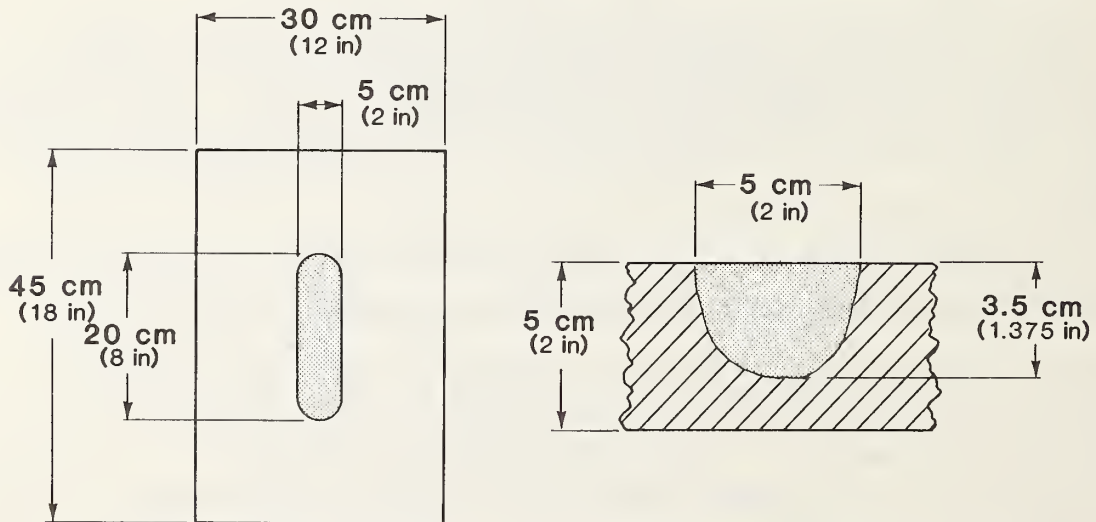


Figure 2. Geometry of the standard Navy trough weld designed by David Taylor Naval Ship Research and Development Center.

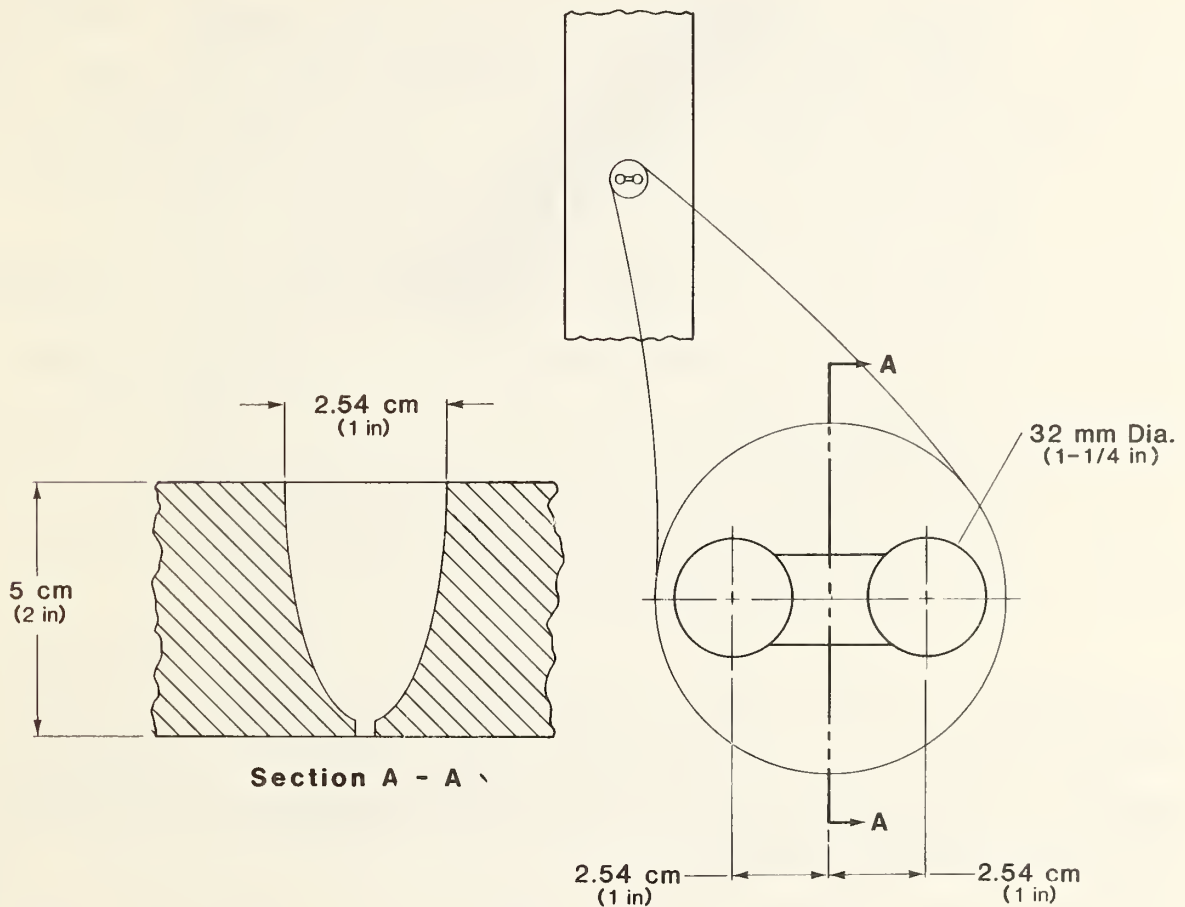


Figure 3. Geometry of a simulated tube-hole-ligament repair weld.

4.1 Wide Plates

The wide-plate geometries are indicated in figure 1. Trough welds (fig. 2) were made in two wide plates, one weld in each plate. One of these plates received PWHT, the other did not; both were tested by the same procedure. Ultrasonic scans were taken before and after welding and after PWHT to determine residual stresses. This technique was successful in the case of the AW plate but inconclusive after PWHT, because the microstructural changes produced by PWHT altered the ultrasound velocities by amounts comparable to the residual stress effects. See Appendix B.

Simulated tube-hole-ligament repairs were made in two plates. Details of the weld geometry are given in figure 3. One plate was given a PWHT, and the other was not. Each test plate was instrumented with strain gages; the strain-gage layouts are given in Appendix C. A part-through surface notch (an artificial crack) was cut into the wide plate with a special saw made for this program. The special saw was needed to produce a notch of the desired geometry without interfering with the strain gages. It used a circular blade 7 cm (2-3/4 in) in diameter by 0.5 mm (0.02 in) thick. The notches were approximately semi-elliptical, 5 cm (2 in) long at the plate surface and 1 cm (0.4 in) deep at the notch center. The notching process also affects residual stresses in these plates. Cutting relieves residual stresses adjacent to the cut; the amount of strain relaxation is related to the magnitude of the residual stress. Residual stress values are derived from measured strains in Appendix C.

After application of additional strain gages, each plate was fatigued in bending in a 1-MN (222-klbf) servohydraulic testing machine, to provide an ideally sharp crack. Each specimen was then tested quasi-statically in four-point bending until failure or until the displacement capacity of the testing facility was exhausted.

4.2 Standard Specimens

Four trough welds, two in each of two plates, were made and then machined into conventional small specimens. These plates were 45 cm (18 in) long by 60 cm (24 in) wide. The troughs were positioned as shown in figure 1. Two of the trough welds received PWHT and two did not. The plan for specimen extraction from each of these welds is shown in figure 4. These plates yielded a total of sixteen bend-bar specimens (5 cm by 2.5 cm; 2 in by 1 in) for J-integral fracture toughness measurements, six round-bar tensile specimens, and fifteen Charpy-impact specimens. The AW weld metal was much harder, more difficult to machine, and wore out the tools much faster than the PWHT weld metal.

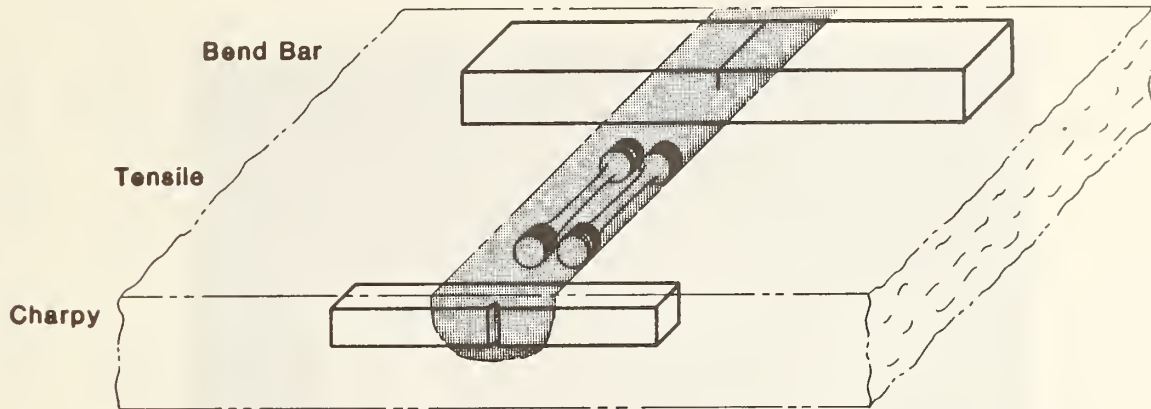


Figure 4. Plan for extraction of standard three-point-bend fracture toughness, Charpy, and round tensile specimens from trough welds.

5. EXPERIMENTAL RESULTS

Experimental results indicate clear and significant differences between the properties of simulated repair welds with and without PWHT. The welds with PWHT have a much higher toughness and a lower yield strength. Furthermore, the crack-driving force produced by the residual stresses in the AW plates is comparable to the base-metal and HAZ toughness values. The PWHT relieves the residual stresses and reduces the crack-driving force to negligible levels.

5.1 Weldment Characterization

Sections cut through the trough welds of fractured AW and PWHT specimens were examined metallographically, and their hardness was tested. Figure 5 shows a metallographic section of a trough weld in the AW condition. The Knoop microhardness and the Rockwell hardness of the AW weld metal were considerably higher than that of the PWHT weld metal. Repeated microhardness traverses revealed no hardness peak at the HAZ in either case (fig. 6).

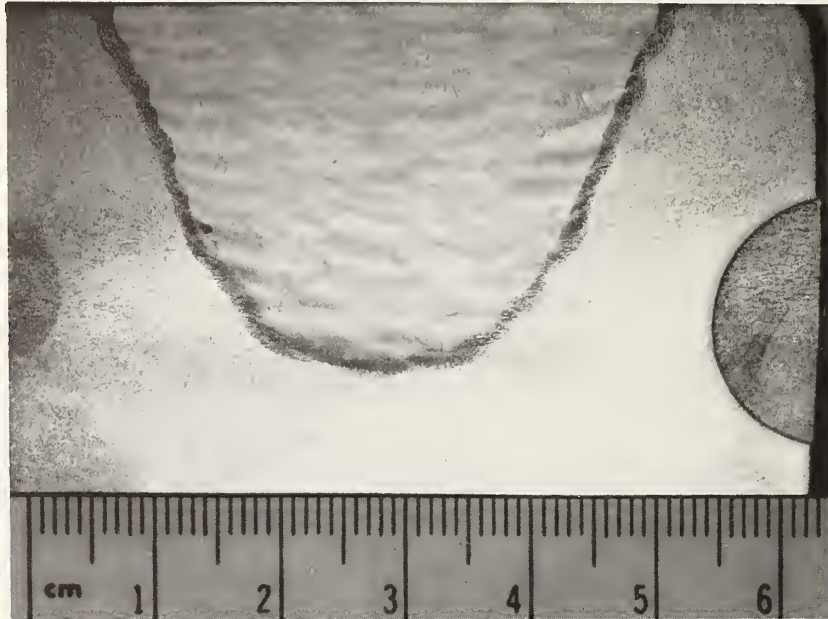


Figure 5. Microstructure of an AW trough weld, near the end.

Note that Charpy impact tests were conducted to determine the transition temperatures for the AW and PWHT weld metal. The results (fig. 7) show that the 54-J (40-ft·lbf) transition temperature of the AW specimens is about 10°C (50°F), and that of the PWHT specimens is about -68°C (-90°F).

5.2 Wide-Plate Results

Two wide-plate tests were run on trough-welded wide plates. Brittle fracture in the form of an extremely large pop-in was observed in the AW plate at a high applied J-value. As is typical, pop-in was marked by a sharp noise, a sudden drop in the measured load, and a sudden increase in the crack-mouth-opening displacement (CMOD), indicating that the crack had suddenly advanced into the specimen. The records of load versus CMOD are reproduced in figure 8. The sizes of the starter crack and the pop-in are shown in figure 9. Examination of the fatigue-marked crack in the AW plate indicated no stable crack growth.

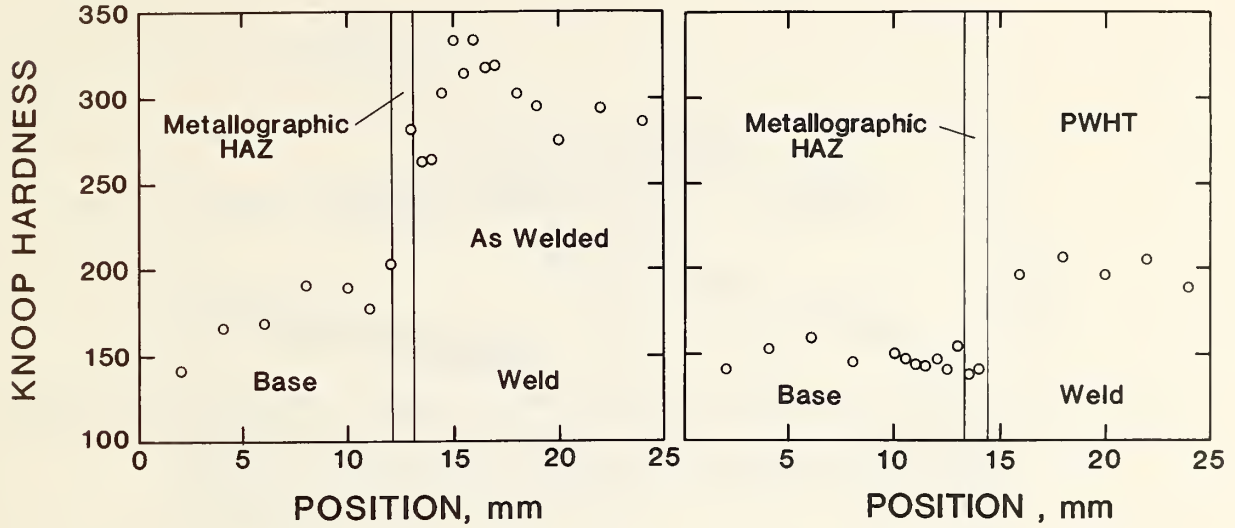


Figure 6. Knoop microhardness as a function of location near the fusion line, AW and PWHT.

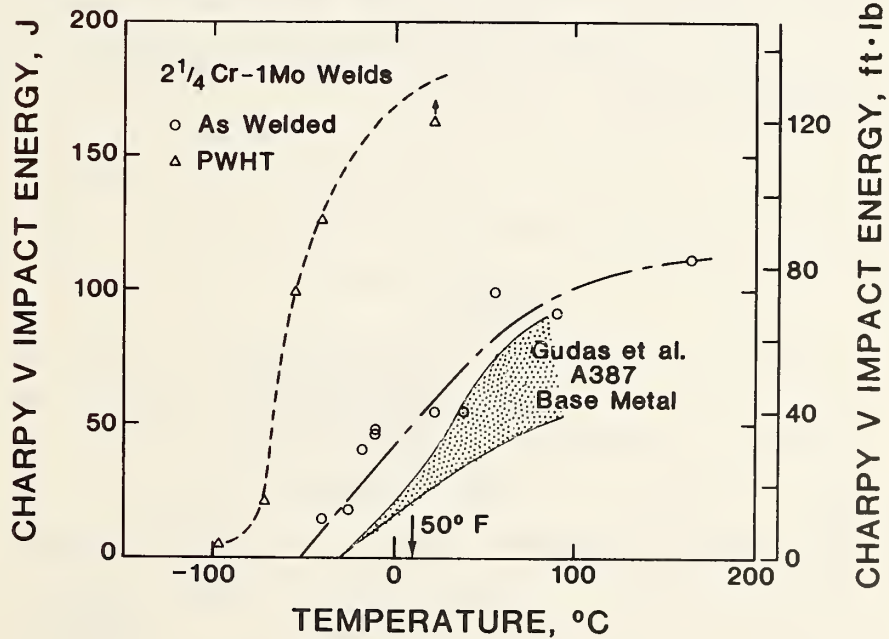


Figure 7. Charpy-V impact-energy transition curves for AW and PWHT weld metal.

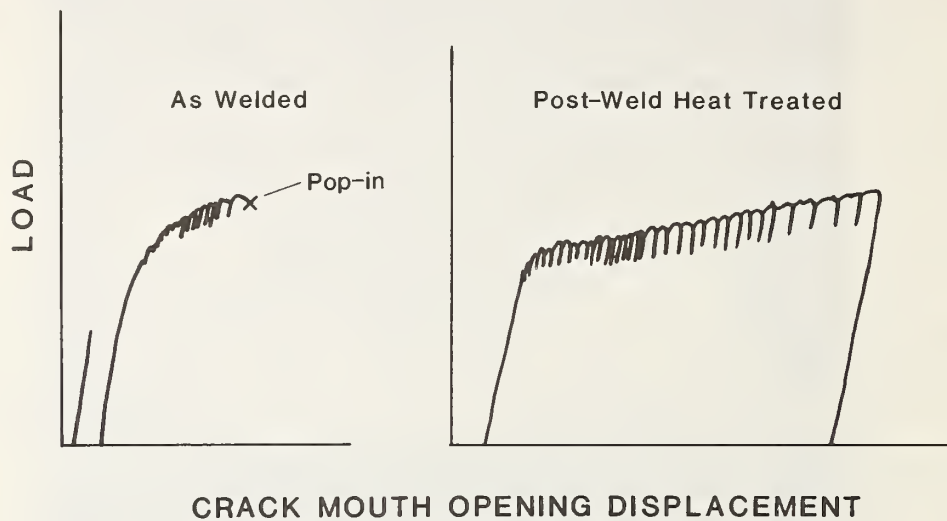


Figure 8. Load-displacement trace for a wide-plate specimen with a semi-elliptical surface crack in an AW trough weld, showing a large pop-in, compared with the load-displacement trace for a wide-plate specimen with a crack in a PWHT trough weld, showing no brittle fracture.

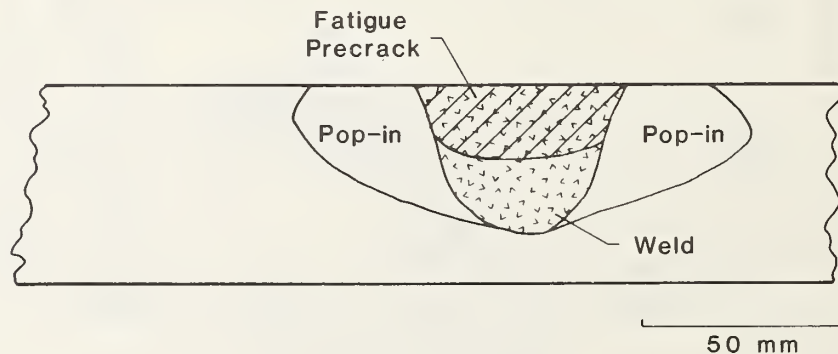


Figure 9. Schematic diagram of the wide-plate fracture surface with the crack in the AW trough weld, showing the extent of the pop-in. The weld was tested in four-point bending at room temperature.

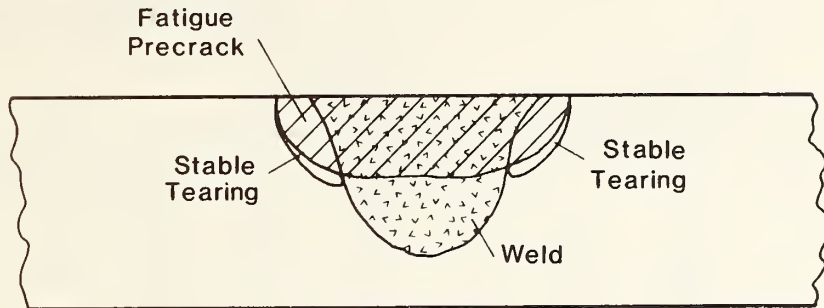


Figure 10. Schematic diagram of the wide-plate fracture surface with the crack in the PWHT trough weld, showing fracturing in the base metal. The weld was tested in four-point bending at room temperature.

A schematic drawing of the fracture surface of the PWHT plate is shown for comparison in figure 10. No macroscopic brittle fracture was observed during the test. The fracture surface contained a small region of apparently brittle fracture in the base metal adjacent to the weld, but no fracture in the weld metal. This was consistent with the standard-specimen tests, because the crack-driving force in the wide-plate tests did not reach the high-toughness values observed for the weld metal in the standard-specimen tests. It also showed that the PWHT weld metal was more fracture resistant than the base metal, consistent with results of standard bend-bar tests.

Two tests were run on wide plates with simulated tube-hole-ligament repairs. The load-displacement traces are compared in figure 11. Brittle fracture in the form of four audible pop-ins was observed in the AW plate. The first pop-in occurred at a J-value consistent with the toughness of the standard specimens. However, the ligament did not fracture through, and the test was continued. Three more pop-ins were observed at higher J-values. Post-test examination showed that the four pop-ins resulted in a crack extension of 11 mm (7/16 in) through the ligament thickness.

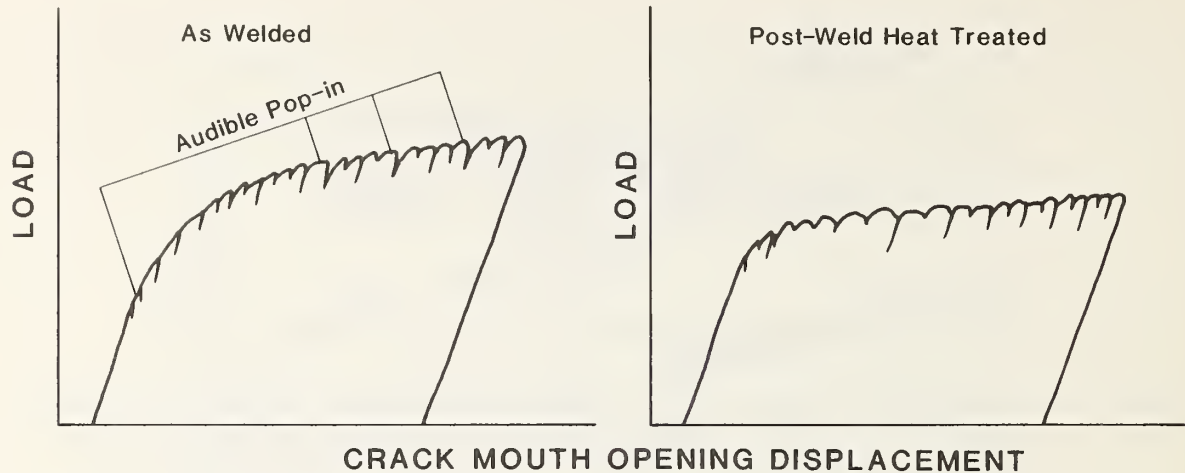


Figure 11. Comparison of the load-displacement trace for a wide-plate specimen with a crack in a simulated AW tube-hole-ligament repair weld (with audible pop-ins noted) with the load-displacement trace for a wide-plate specimen with a crack in a simulated PWHT tube-hole-ligament repair weld, where no pop-ins occurred.

5.3 *J-Integral Fracture-Toughness Tests*

The results of 31 fracture-toughness tests are listed in table 2. High initiation toughness values followed by stable crack growth were observed in the two tests of PWHT weld metal. The average initiation toughness level was 536 kN/m (3060 lbf/in). After initiation, the crack growth resistance of the PWHT weld metal was very high, practically indistinguishable from the resistance curve associated with crack blunting. In four tests of AW weld metal, the average initiation toughness value was 87 kN/m (478 lbf/in). Unstable crack propagation, in the form of repeated pop-ins followed by brittle fracture of the whole specimen, was observed in all the AW weld-metal specimens tested.

Eight tests were performed on specimens with cracks located in the heat-affected zone (HAZ), four with PWHT welds and four with AW welds. The results of these tests indicate that the HAZs in both PWHT and AW welds

Postweld Heat Treatment Criteria

Table 2. Fracture Toughness Values for Standard Trough Welds
in 2½Cr-1Mo Plate

Specimen Number	Notch Location	Condi- tion	a/W	J-Integral			CTOD			K(J _C) MPa/m	or K(δ _C) ksi/in
				J Criterion	J kN/m	J lbf/in	δ Criterion	δ mm	δ in · 10 ⁻³		
1NJ1	WM	AW	0.51	J _C	68.3	397	δ _C	0.077	3.0	123	112
1NJ2	WM	AW	0.52	J _C	77.9	445	δ _C	0.086	3.4	131	119
2NJ1	WM	AW	0.51	J _C	138	789	δ _C	0.132	5.2	174	158
2NJ2	WM	AW	0.51	J _C	122	694	δ _C	0.104	4.1	164	149
1SJ1	WM	PWHT	0.51	J _{IC}	415	2370	δ _i	0.521	20.5	302	275
1SJ2	WM	PWHT	0.53	J _{IC}	245	1400	δ _i	0.307	12.1	232	211
1SJ4	WM	PWHT	0.53	J _m	869	4960	δ _m	1.10	43.2	437	398
2SJ2	WM	PWHT	0.48	J _{IC}	569	3250	δ _i	0.673	26.5	354	322
1NJ3†	HAZ	AW	0.45	J _C	38.0	217	δ _C	0.0549	2.16	91	83
2NJ3	HAZ	AW	0.44	J _C	5.25	30.0	δ _C	0.0053	0.21	34	31
CMALC3	HAZ	AW	0.54	J _C	14.4	82.4	δ _C	0.0272	1.07	55	50
CMALC4	HAZ	AW	0.43	J _C	8.84	50.5	δ _C	0.0130	0.51	44	40
CMALC5	HAZ	AW	0.50	J _C	5.67	32.4	δ _C	0.0068	0.27	35	32
2SJ1	HAZ	PWHT	0.50	J _C	39.8	227	δ _C	0.082	3.2	94	85
2SJ3	HAZ	PWHT	0.48	J _C	50.8	290	δ _C	0.090	3.6	106	96
2SJ4	HAZ	PWHT	0.52	J _C	25.7	147	δ _C	0.051	2.0	75	68
1SJ3	HAZ	PWHT	0.46	J _C	32.0	183	δ _C	0.075	2.9	84	76
CMPB5	BM	PWHT	0.54	J _C	65.7	375	δ _C	0.150	5.9	120	109
CMPB6	BM	PWHT	0.54	J _C	167	952	δ _C	0.384	15.1	192	174
CMPB7	BM	PWHT	0.42	J _C	114	650	δ _C	0.259	10.2	158	144
CMPB8	BM	PWHT	0.32	J _C	96.8	553	δ _C	0.244	9.6	146	133
CMPB9	BM	PWHT	0.44	J _C	98.9	565	δ _C	0.253	10.0	147	134
CMPB10	BM	PWHT	0.25	J _C	67.1	383	δ _C	0.220	8.6	121	111
CMPB11	BM	PWHT	0.27	J _C	101	579	δ _C	0.279	11.0	149	136
CMPB13	BM	PWHT	0.14	J _u	496	2830	δ _u	1.32	52.1	330	300
CMPB14	BM	PWHT	0.65	—	—	—	δ _C	0.094	3.7	80	73
CMPB15	BM	PWHT	0.34	—	—	—	δ _C	0.43	16.9	171	156
CMPB16	BM	PWHT	0.14	J _u	427	2440	δ _u	1.12	44.0	306	279
CMPB17	BM	PWHT	0.10	—	—	—	δ _u	0.49	19.3	183	166
1NJ4	BM	AW	0.51	J _C	41.2	235	δ _C	0.089	3.5	95	87
2NJ4	BM	AW	0.50	J _C	40.1	229	δ _C	0.087	3.4	94	85

† Out-of-plane crack growth.

WM = weld metal; HAZ = heat-affected zone; BM = base metal; AW = as welded;
PWHT = post-weld heat treated; CTOD = crack tip opening displacement;
J_C = J-integral measured at a "pop-in"; J_{IC} = fracture toughness for slow,
stable crack growth; J_m = J-integral measured at maximum load; J_u = J-integral
measured at brittle fracture following stable crack growth (J-R curve not available).

are brittle. The PWHT HAZ had an average critical J-value of 47 kN/m (270 lbf/in). The AW HAZ had an average critical J-value of 15 kN/m (87 lbf/in). No stable crack growth was observed in these tests, and the crack in one AW specimen appeared to follow the HAZ instead of going straight.

Two of the base-metal specimens had very low a/W ratios, which caused the final J-value to be very high at failure. These two tests were not included in the calculation of the average toughness values.

5.4 Tensile Tests

Triplicate tensile tests of round-bar tensile specimens, 6.2 mm (0.25 in) in diameter, indicated that the weld metal before PWHT is significantly stronger than both the base metal and the PWHT weld metal. The results are listed in table 3. For AW weld metal, the yield strength was 767 MPa (111 ksi) and the ultimate strength was 843 MPa (122 ksi); for the PWHT weld metal, the yield strength was 454 MPa (66 ksi) and the ultimate strength was 579 MPa (84 ksi). According to the manufacturer, the yield strength of the base plate was 270 MPa (39 ksi), and the ultimate strength was 499 MPa (72 ksi). The weld metal in the AW and PWHT conditions had similar ductilities.

Table 3. Tensile Properties for Standard Trough Welds in 2½Cr-1Mo Plate.

Material	No. Obs.	Yield Strength, MPa (ksi)	Ultimate Strength, MPa (ksi)	Elongation, percent	Reduction of Area, percent
WM-PWHT	2	454 (65.8)	579 (84.0)	28	74
WM-AW	3	767 (111)	843 (122)	23	66

WM = weld metal; PWHT = postweld heat treated; AW = as welded;
 No. Obs. = number of observations

6. RESULTS AND DISCUSSION:

DIRECT MEASUREMENT OF THE J-INTEGRAL IN THE WIDE PLATES

The applied J-integral of the four wide-plate specimens as a function of applied bending stress is shown in figures 12 and 13, the primary experimental results of this series of tests. These figures portray the effect of residual stress and applied bending stress on the crack-driving force, as characterized by the J-integral. The stress values plotted are the elastically calculated outer-fiber tensile stresses for the wide-plate specimen

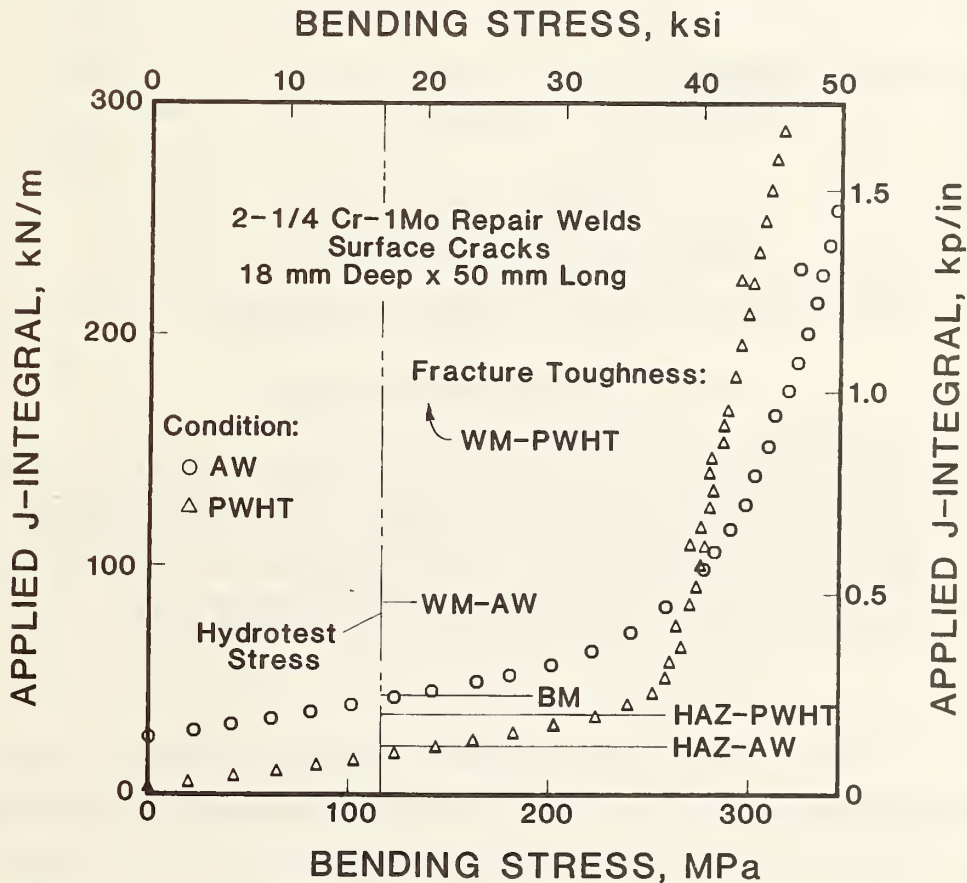


Figure 12. Applied J-integral as a function of imposed bending stress for the AW and PWHT wide-plate specimens with surface cracks in trough welds. The vertical line marks a convenient stress level approximating the stress near a tube hole during a maximum-pressure hydrostatic test. Relevant toughness levels are indicated by horizontal lines.

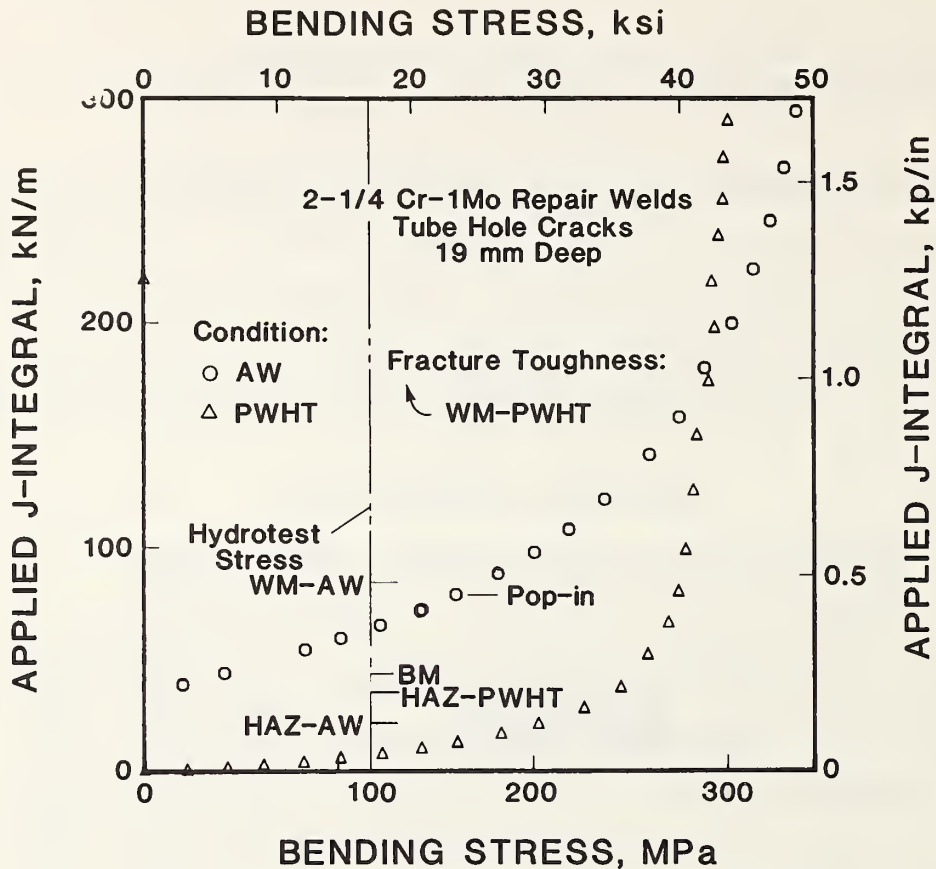


Figure 13. Applied J-integral as a function of imposed bending stress for the AW and PWHT wide-plate specimens with surface cracks in simulated tube-hole-ligament repair welds. The vertical line marks a convenient stress level approximating the stress near a tube hole during a maximum-pressure hydrostatic test. Relevant toughness levels are indicated by horizontal lines.

loaded in four-point bending. For the PWHT specimens, J-value was close to zero for zero bending stress. As the stress was increased, J increased gradually. When the stress reached approximately the yield strength of the base plate, plastic strain became significant. The applied J-integral increased along with the plastic strains, whereas the stress stayed nearly constant.

For the AW specimen, residual stresses caused a significant level of crack-driving force even before the bending stress was applied. The J-integral increased gradually with the bending stress. When the stress reached an effective yield strength, plastic strain became significant, and the J-integral increased rapidly with stress. The effective yield strength of the AW plate was higher than that of the PWHT plate because of the higher yield strength of the AW weld metal.

For the AW plate with the surface crack in the trough weld, the pop-in indicated in figure 8 occurred at a J-level of about 275 kN/m (1570 lbf/in). This is much higher than the critical J-levels observed in the standard specimen tests, about 87 kN/m (478 lbf/in), but the orientation of the crack relative to the weld was different. In the wide plate, the crack was perpendicular to the weld, whereas in the standard specimen, the crack was parallel to the weld. The observed results indicate the possibility of an orientation effect on the weld toughness as well as an effect due to size and geometry.

The effect of the residual stresses on applied J for both PWHT and AW plates was calculated by including in the applied analysis residual strains equal to the measured strain relaxation when the notch was cut. This is the first known use of this technique. The results (figs. 12 and 13) show that the residual stress-strains raise the applied J-levels by 20 to 30 kN/m (114 to 171 lbf/in), for the cracks tested. This increase is especially significant when considered in conjunction with the low toughness values of the base metal and HAZ, which are noted in the figures.

The rather low values of the AW-HAZ toughness compared with the moderate applied J-values produced by the residual stresses stimulated interest in the applied J-values as a function of notch depth. Because strains and crack depths had been recorded continuously during the cutting process, the data needed were available. Applied J was calculated at each crack depth. The results are shown in figure 14.

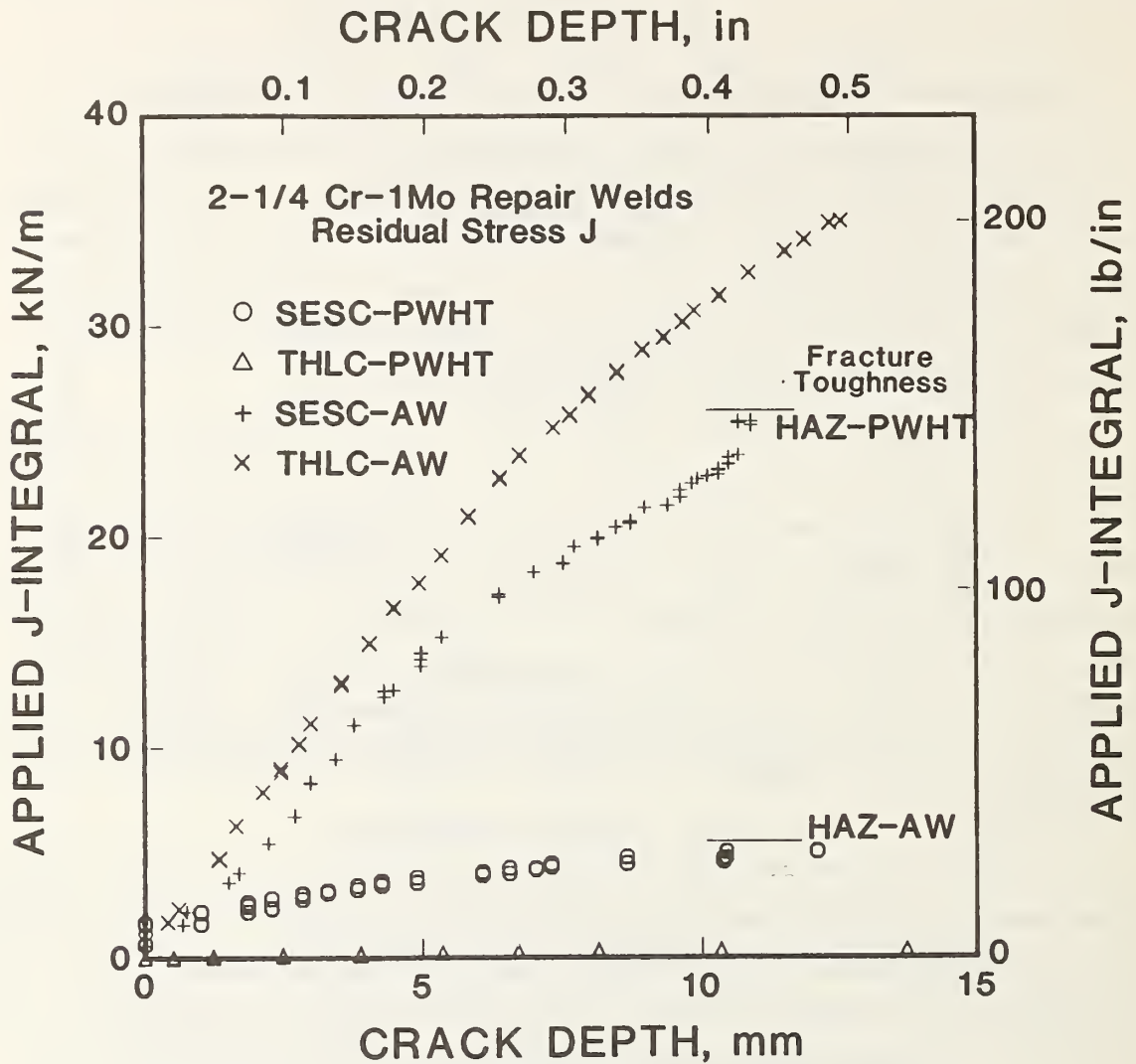


Figure 14. Applied J-integral as a function of cut depth for the AW and PWHT wide-plate specimens with semielliptical surface cracks (SESC) in trough welds and in simulated tube-hole-ligament-crack (THLC) repair welds. For comparison, the mean toughness, 15 kN/m (187 lbf/in), of the AW-HAZ is indicated by the horizontal line labeled *Fracture Toughness: AW-HAZ* near the left side of the plot.

7. IMPLICATIONS

These experimental results of 2½Cr-1Mo repair welds indicate that the PWHT of the current weld consumable is definitely beneficial. The major benefit is a much higher fracture resistance in PWHT weld metal than in the AW weld metal. Reduction of residual stresses is another advantage.

Figures 12 and 13 compare the measured toughness values to the applied J-integral at a selected stress value corresponding to an estimated maximum hydrotest stress near a tube hole. The hydrotest stress is indicated by the vertical line in each figure; the toughness levels are indicated by horizontal bars. If the toughness is less than the applied J, fracture is predicted. The toughness of the PWHT weld metal is above the range of these plots. These figures indicate that the PWHT and AW weld metals are tough enough to prevent fracture at the crack sizes used in these tests. The base-metal and PWHT-HAZ toughness values are above the PWHT driving-force curves, indicating a safe condition. However, the AW-HAZ and base-metal toughness values are below the AW driving-force curve, indicating the possibility of fracture. Linear scaling of the test crack sizes indicated that a safe condition could be reached by limiting the crack sizes to about 5 mm (0.2 in). This estimated critical crack size was refined by using the data of figure 14, which plots applied J-integral against crack depth for PWHT and AW wide plates. The crack depths correspond to the depths of the saw cut when cutting was interrupted to record strains from strain gages for J-integral calculation. The figure shows that the J-integral increased much more rapidly with crack depth in the AW plates; it reached the toughness of the AW-HAZ at depths of about 5 mm. However, the toughness was measured using standard bend bars.

If it is necessary to omit the PWHT, compensating action should be taken to ensure the safety of the superheater header, such as restricting the omission of PWHT to very shallow welds, so that the possible crack size is limited. Extra-stringent inspection could be required for the AW welds, to ensure that all cracks have been removed. Omission of PWHT could be

restricted to welds in low-stress regions. A special local stress relief of some sort could be developed, which would give sufficient toughness to the weld deposit, but which might not relieve the residual stresses as well as a conventional PWHT. Selection of a different weld-metal consumable for repair welds could be considered as a metallurgical remedy to the nonoptimum properties of the current consumable in the non-PWHT state.

8. NOTE ON THE EXPERIMENTAL APPROACH

The experimental technique of direct measurement of the applied J-integral was developed previously [7]. Some applications to surface flaws have been reported, for example, in reference 8. The behavior of the J-integral in three dimensions was discussed in reference 9, and its behavior in welds is a topic of current research [10].

This is the first report known to the authors of the application of this technique to repair welds and to an evaluation of PWHT. Appendix D, a companion report, gives the details of this technique and its basis. Apparently, this technique can provide valuable data on the applied J-integral in welds. In particular, the data given in figure 14 are unique. Previously, only engineering estimates of the applied J-integral produced by residual stresses have been available. Because this approach is relatively new, the results should be applied with caution.

9. ACKNOWLEDGMENTS

The financial support provided by the Naval Sea Systems Command through project sponsor Commander L. R. Easterling is gratefully acknowledged. Helpful discussions with W. C. Fraser and M. A. E. Natishan of the David Taylor Naval Ship Research and Development Center are appreciated. Technical assistance by J. D. McColskey, M. Moyer, and J. J. Broz of the National Bureau of Standards is also appreciated.

10. REFERENCES

- [1] Naval Sea Systems Command. Military standard: fabrication welding and inspection; and casting inspection and repair for machinery, piping, and pressure vessels in ships of the United States Navy. MIL-STD-278E(SH), Department of the Navy, Washington, D.C.; 1976.
- [2] Lundin, C.D., Kruse, B.J., and Pendley, M.R. High temperature properties of 2-1/4 Cr 1 Mo weld metal. Weld. Res. Council. Bull. 277, May 1976, pp. 1-27.
- [3] Swift, R.A. and Rogers, H.C. Embrittlement of 2-1/4 Cr-1 Mo steel weld metal by postweld heat treatment. Weld. J. - Res. Suppl., April 1973, pp. 145s-153s.
- [4] Greene, T.W. Evaluation of the effect of residual stresses. Weld. J. - Res. Suppl., May 1949, pp. 193s-204s.
- [5] Gudas, J.P., Zanis, C.A., Czyryea, E.J., Franke, G.L., Hackett, E.M., and Palko, W.A. Fitness for service analysis of defects in the USS Saratoga (CV-60) superheater headers. DTNSRDC/SME-83/62, David Taylor Naval Ship Research and Development Center, Annapolis, Maryland, August 1983.
- [6] Blackburn, J.M. The weldability and properties of 2-1/4% chromium - 1% molybdenum steel used for Navy ship boiler components - A literature review. (Distribution limited to U.S. Government agencies only.) DTNSRDC/SME-84/146, David Taylor Naval Ship Research and Development Center, Annapolis, Maryland, January 1985, 58 pp.
- [7] Read, D.T. Experimental method for direct evaluation of the J-contour integral, in Fracture Mechanics: Fourteenth Symposium - Volume II: Testing and Applications. J.C. Lewis and G. Sines, Eds. ASTM STP 791, American Society for Testing and Materials, Philadelphia, 1983, pp. II-199-II-213.
- [8] King, R.B., Cheng, Y.W., Read, D.T., and McHenry, H.I. J-integral analysis of surface cracks in steel plates, in Elastic-Plastic Fracture: Second Symposium, Volume I - Inelastic Crack Analysis. C.F. Shih and J.P. Gudas, Eds. ASTM STP 803, American Society for Testing and Materials, Philadelphia, 1983, pp. I-444-I-457.
- [9] Carpenter, W.C., Read, D.T., and Dodds, R.H., Jr. Comparison of several path independent integrals including plasticity effects. Int. J. Fract. 31, 1986, pp. 303-323.

- [10] Read, D.T. Experimental results for fitness-for-service assessment of HY130 weldments. NBSIR 84-1699, National Bureau of Standards, Boulder, Colorado, March 1984.

APPENDIX A. DESCRIPTION OF THE WELDING PROCEDURE

T. A. Siewert

All elements of the welding procedure were chosen in consultation with the David Taylor Naval Ship Research and Development Laboratories (DTNSRDL) in an attempt to reproduce the field welding conditions.

The weld joints had been machined; therefore, no grinding was needed to remove surface oxides or surface irregularities. However, the joint regions were carefully degreased to remove residual machine lubricants. The final step before welding was preheating the plate to 205°C (400°F). The plate was maintained between 205° and 260°C (400° and 500°F) until the weld was completed and then allowed to cool slowly.

Welding was performed using a 2.4-mm (3/32-in) diameter MIL 9018-B3L electrode conforming to MIL-E-22200/8B. At 80 A and with a weave of about one electrode diameter, each electrode produced about 10 cm (4 in) of weld bead and a heat input of 1 kJ/mm (24 kJ/in). A new 4.5-kg (10-lb) hermetically sealed can of electrodes was used for each weld to keep hydrogen potential low.

All these procedural details were kept constant for all welds. The pass-layer sequence was different for the two types of weld joint, but was kept constant for each type.

The DTNSRDC standard joint geometry was a boat-shaped weld about 20 cm (8 in) long, 5 cm (2 in) wide, 3.3 cm (1.3 in) deep, and with a rounded bottom. Since each pass required two electrodes, there was a possibility of differing microstructure or weld flaws in the intermediate start-stop region. To minimize the effects of this variable on the property measurements, all the intermediate starts and stops occurred within 1 cm of the centerline, and this region was avoided in the mechanical testing program. Each layer near the bottom of the trough contained two passes; the top layer had five or six passes. These welds contained between 16 and 18 layers for an average number of passes near 85 (170 electrodes).

The second joint geometry simulated the repair of a through-wall crack in the ligament between two boiler tube holes. The joint was about 2.5 cm (1 in) wide near the top, about 0.3 cm (0.12 in) wide near the bottom, and was about 5 cm (2 in) in length. Here, each pass could be completed with a single electrode. Start and stop regions were inside the tube bore so they would be removed during the subsequent remachining of the tube bore. Each layer near the bottom contained one pass; layers near the top had four passes. These welds contained 19 to 22 layers for an average number of beads near 58.

APPENDIX B. ULTRASONIC MEASUREMENTS OF RESIDUAL STRESS

A. V. Clark

Ultrasonic measurements of residual stresses were made using electromagnetic-acoustic transducers (EMATs). Since the EMATs are noncontacting, we can measure the arrival times of ultrasonic waves at locations of interest before the plates are welded and then remeasure arrival times at the same locations after welding. If (a) liftoff effects are negligible, (b) plate thickness changes are due solely to elastic strains, and (c) no microstructural changes occur, then changes in arrival times are due solely to stress.

Mathematically, we have

$$\frac{\Delta t_x}{t_x} = - (a\sigma_{xx} + b\sigma_{yy}) \quad (\text{B1a})$$

$$\frac{\Delta t_y}{t_y} = - (a\sigma_{yy} + b\sigma_{xx}) \quad (\text{B1b})$$

where a and b are constant and Δt_x is the difference of arrival times before and after welding, with EMATs polarized in the σ_x -direction. (We here assume that the principal stresses σ_x and σ_y act along material symmetry axes.) If $a^2 \neq b^2$, then σ_x and σ_y can be determined by inverting the two equations above.

Because of the cavity geometry and the welding pass sequence, we expect the stress to have a complicated variation in the plate thickness direction. We make the simplifying assumption that stresses σ_{xx} and σ_{yy} are caused mainly by transverse and longitudinal shrinkage of weld metal, respectively. Consequently, we expect that σ_{xx} will be composed of both a bending and a membrane stress, because there will be more shrinkage of weld metal at the top of the cavity than at the bottom. We also expect σ_{yy} to be primarily a membrane stress (constant through the plate thickness). Our ultrasonic technique measures the thickness-averaged stresses.

Arrival times were measured along the plate centerline before and after welding (with temperature compensation). Equation B1 was used to calculate σ_{xx} and σ_{yy} outside the weld. These values are shown in figure B1.

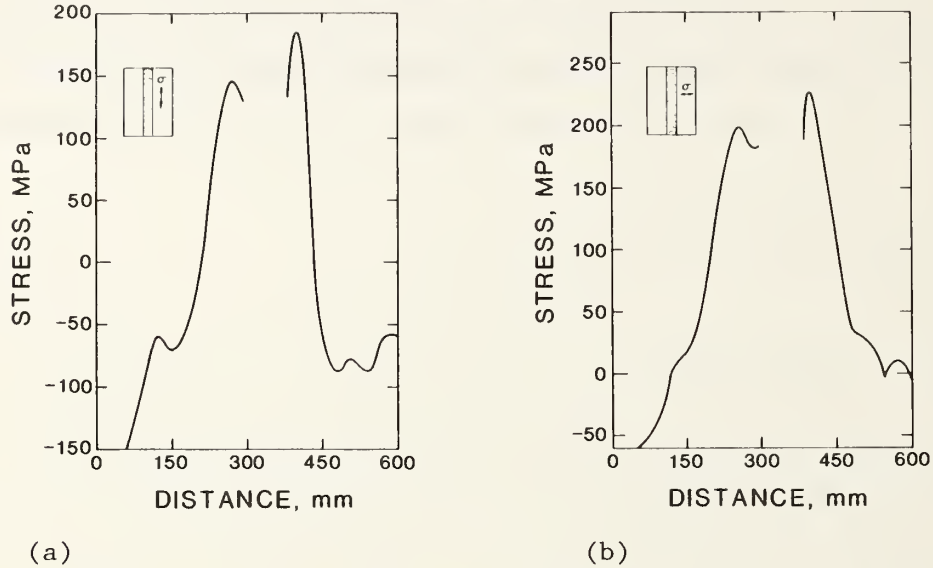


Figure B1. Residual stress, measured ultrasonically, as a function of position near a trough weld in a wide plate, (a) along the weld and (b) across the weld.

To obtain the longitudinal stress inside the weld, we use the self-equilibrating nature of residual stress to give

$$\int_{-L}^L \sigma_{yy} dx = 0. \quad (B2)$$

where $2L$ is the plate width. We calculated $\int \sigma_{yy} dx$ outside the weld, and assumed that σ_{yy} is a constant inside the weld. We found that in order for equation B2 to be satisfied, we have $\sigma_{yy} = 380$ MPa inside the weld.

D. T. Read

Residual stresses are eliminated by mechanical relaxation when the associated force paths are cut. This principle is the basis of the standard method of determining residual stress by drilling a hole near strain gages. The strain gages measure the relaxation that occurs during drilling; the residual stress level is calculated from these relaxations. This same principle allows calculation of residual stress perpendicular to a cut from strain relaxations measured during cutting.

Figure C1 shows the strain-gage layout used on the front side and back side of the plate. The gages along the weld axis provide checks on the paired gages near the cut and are used in J-integral calculations. Figure C2 displays a plot of strain relaxation 7 mm (0.28 in) from the cut as a function of cut depth. The strain relaxation is nearly complete at a cut depth of 8 mm (0.31). Gages nearer to the cut saturate at lower depths, and vice versa. Figure C3 shows that strain relaxation decreases as distance from the cut increases (circles). The magnitude of the relaxation of strains parallel to the cut is also plotted (squares).

The complex dependence of strain on distance from the cut in the AW plate is shown in figure C4. Instead of a uniform exponential decay with distance from the cut, which would appear as a straight line when plotted in semilogarithmic coordinates, figure C4 shows that the relaxation strains are nearly constant near the cut and then decay further away. Figure C5 shows the behavior near the cut in more detail. Figures C6 and C7 show the behavior of the PWHT plate, where an exponential decay of strain with distance occurred at distances up to 20 mm. The specific reason for this difference between the AW and PWHT plates is not known.

The same sort of difference between AW and PWHT welds was observed in the simulated tube-hole-ligament repair welds (figs. C8 through C10). Figure C11 shows strain relaxations measured on the bottom side of one PWHT and one AW plate. These were small, so only the strain directly opposite the cut was measured in subsequent tests.

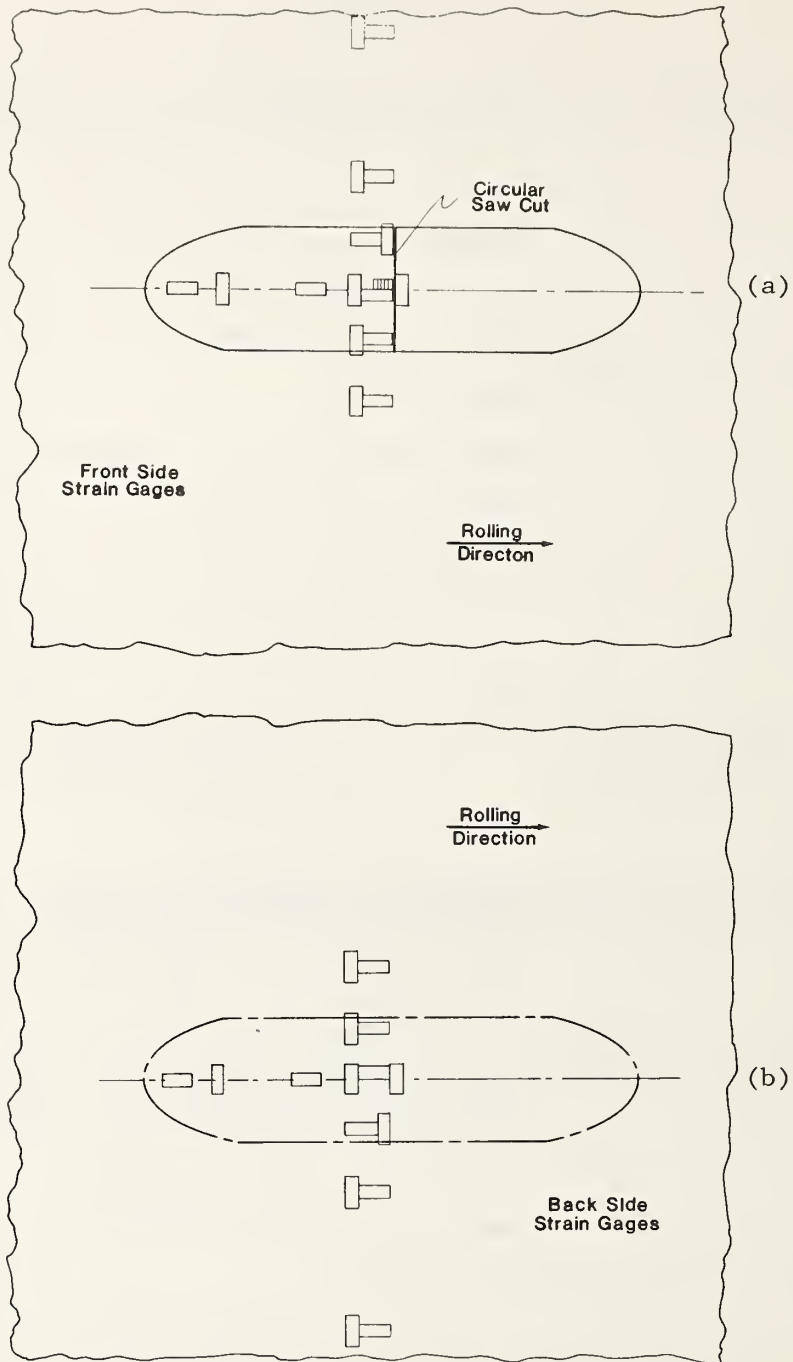


Figure C1. Strain-gage layout for measurement of residual strain relaxation during the cutting of the notch; (a) front-side strain, (b) back-side strain.

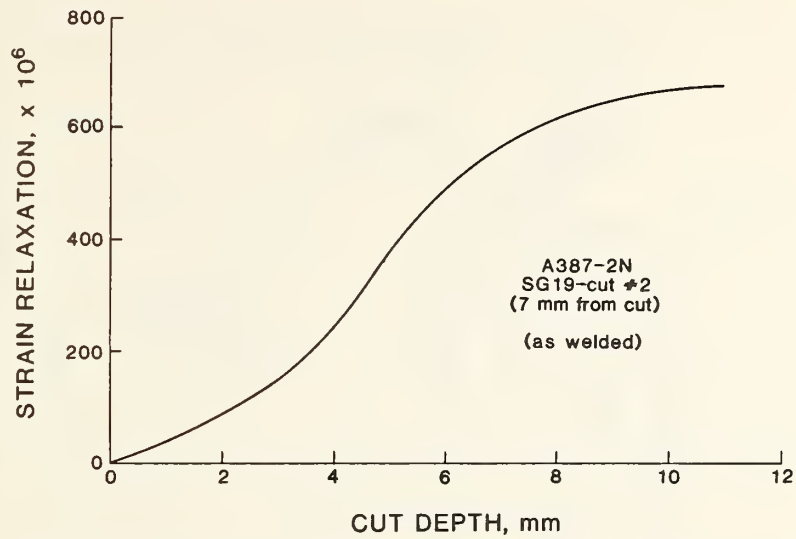


Figure C2. Strain relaxation measured by a gage centered 7 mm (0.28 in) from the semicircular cut in an AW trough weld, as a function of cut depth.

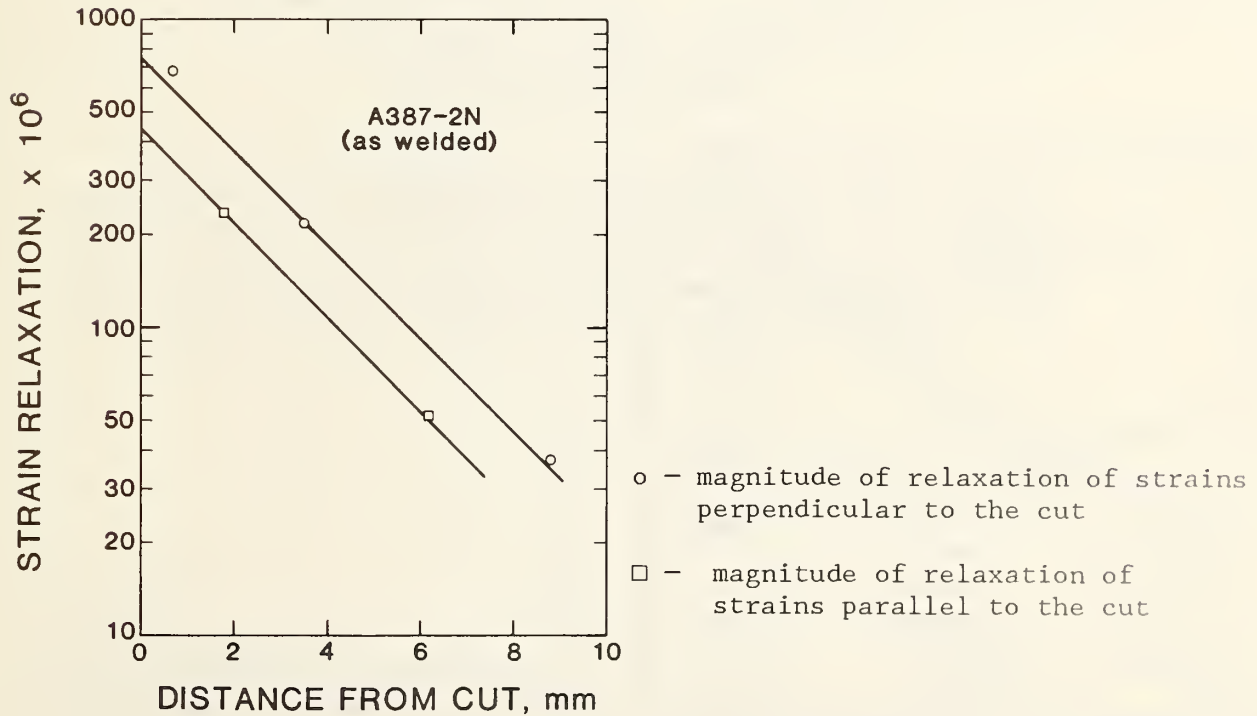


Figure C3. Strain relaxation in specimen 2N as a function of distance from the cut at a depth of 11 mm (0.43 in).

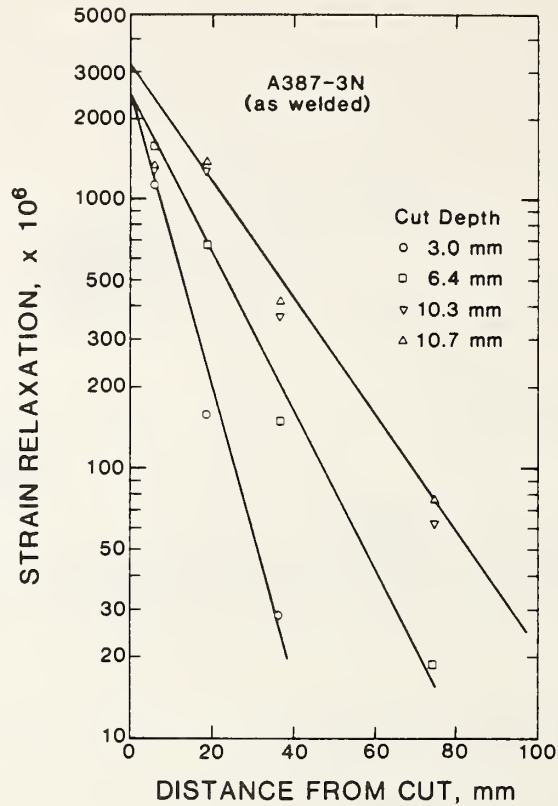


Figure C4. Strain relaxation as a function of distance from the semi-circular cut in trough weld in AW specimen 3N for several cut depths. Each of the symbols at 4 mm (0.16 in) from the cut represents an approximate average, excluding outliers, of the maximum strains from an array of small strain gages near the cut. The actual data from these gages are shown in figure C5.

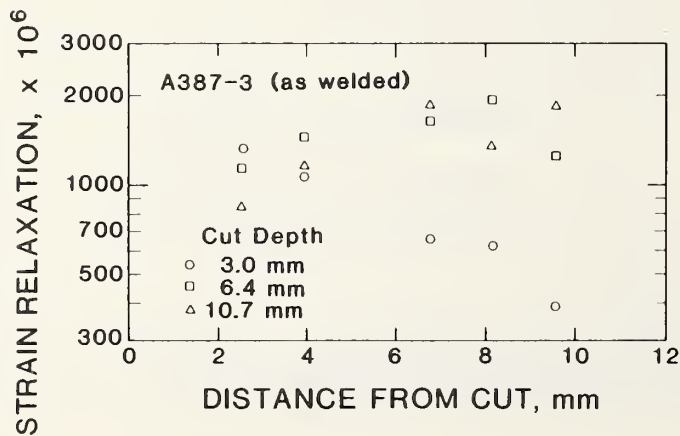


Figure C5. Strain relaxation as a function of distance near the cut in an AW trough weld of specimen 3N, for several cut depths.

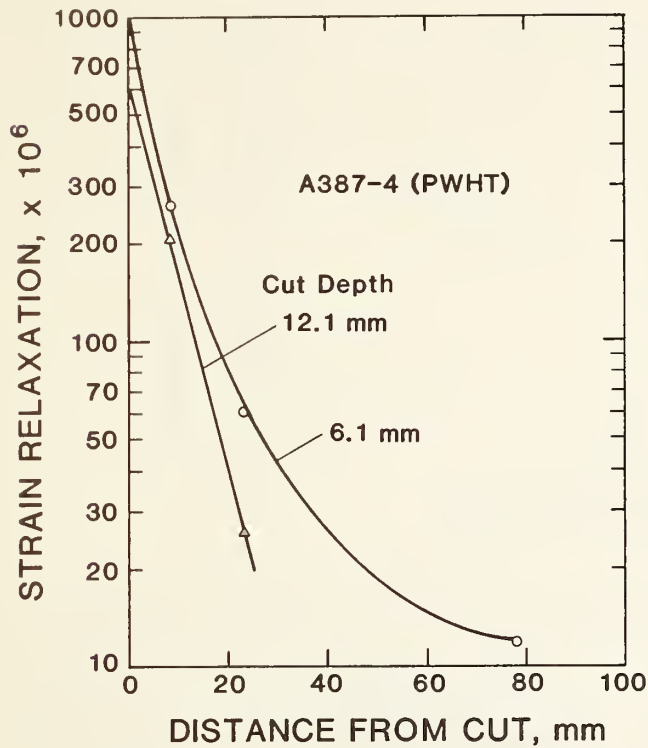


Figure C6.

Strain relaxation as a function of distance from the semicircular cut in a trough weld in PWHT specimen 4 for two cut depths.

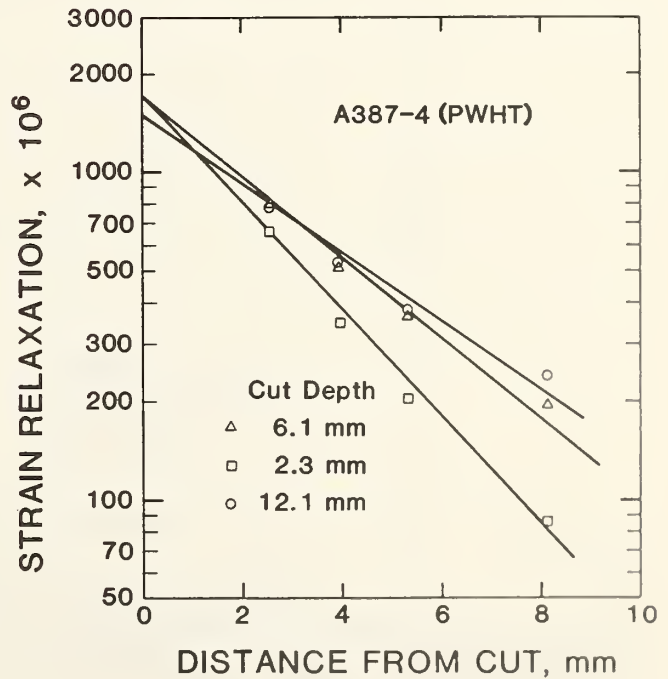


Figure C7.

Strain relaxation as a function of distance near the cut in a trough weld in PWHT Specimen 4 for three cut depths.

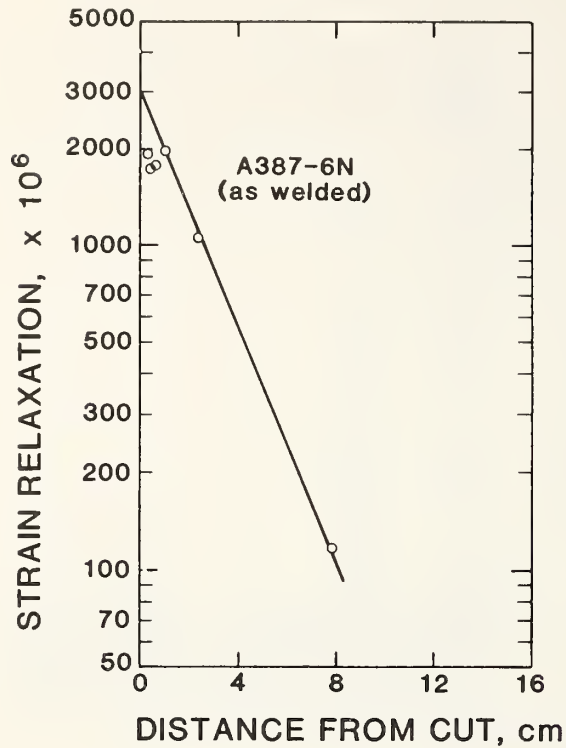
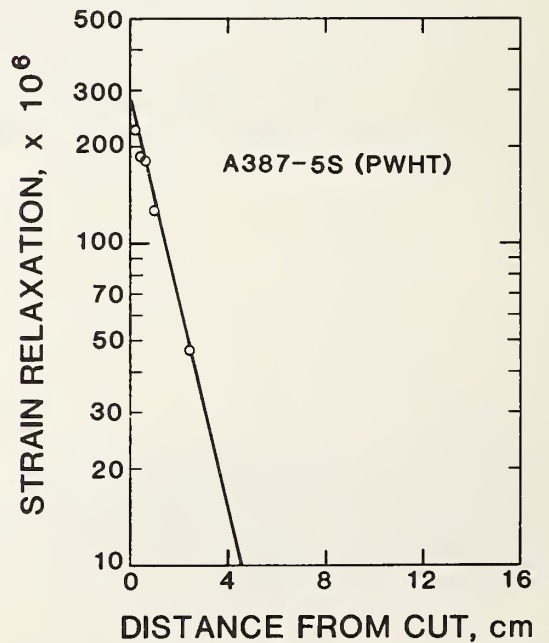


Figure C8.

Strain relaxation as a function of distance from the cut in a simulated tube-hole-ligament repair weld of AW specimen 6N.

Figure C9.

Strain relaxation as a function of distance from the cut in a simulated tube-hole-ligament repair weld of PWHT specimen 5S.



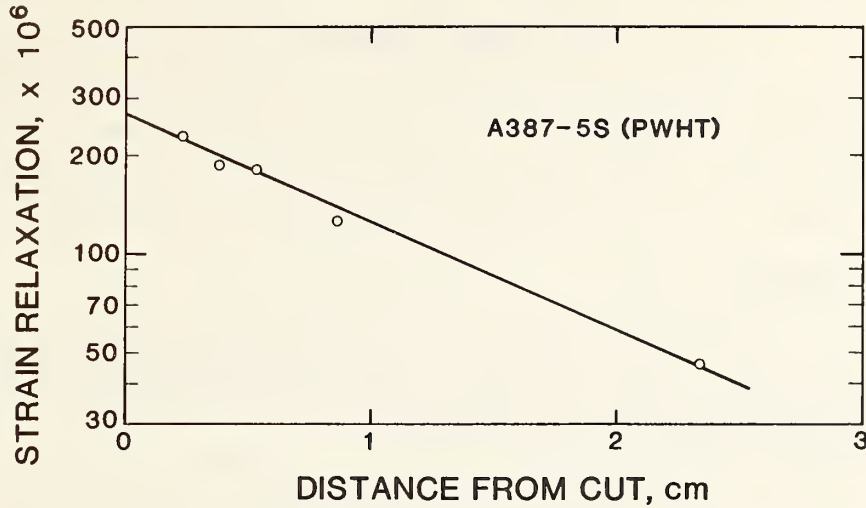


Figure C10. Strain relaxation as a function of distance near the cut in a simulated tube-hole-ligament repair weld of PWHT specimen 5S.

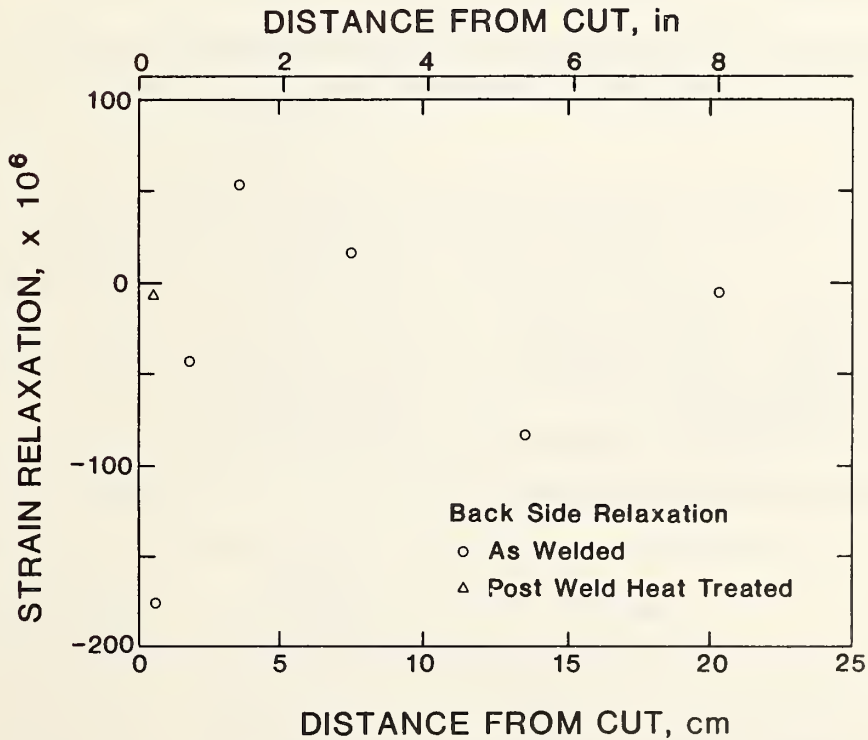


Figure C11. Strain relaxation on the back side as a function of distance from the semicircular cut in two trough welds, AW and PWHT.

The residual strains reported in table C1 represent the extrapolation to the cut position of the strain values measured 2 cm (3/4 in) and farther away from the cut. This extrapolation ignores the saturation effect noted above. The residual stresses represent the average saturated strain value measured near the cuts, multiplied by Young's modulus. The Poisson correction was determined to be insignificant by using data from transversely oriented strain gages.

The residual strains are affected by the PWHT more than the residual stresses (see table C1). The mechanism of this difference and of the noted strain saturation near the cut are unknown.

In the J-integral calculations, the saturated strain values were used, so that the reported values of applied J-integral produced by residual stresses are lower bound values.

Table C1. Residual Stresses at Simulated Repair Welds in Plates of 2½Cr-1Mo Steel.

Standard Troughs

Condition	Method	Stress, MPa (ksi)	Strain (post yield)
PWHT	Strain gage (cutting)	325 (47.1)	1.6×10^{-3}
AW	Strain gage (cutting)	372 (54.0)	2.6×10^{-3}
AW	Ultrasonic	380 (55.1)	-

Simulated Tube-Hole-Ligament Repairs

Condition	Method	Stress MPa (ksi)	Strain (post yield)
PWHT	Strain gage (cutting)	55 (8.0)	0.3×10^{-3}
AW	Strain gage (cutting)	383 (55.5)	2.9×10^{-3}

D. T. Read

INTRODUCTION

A quantitative evaluation of the applied J-integral produced by residual stresses is needed to make decisions on post-weld heat-treatment (PWHT) criteria and inspection criteria based on fitness-for-service (FFS) assessment in structures where fracture must be avoided. Existing FFS assessment procedures typically include a procedure such as adding the residual strain to the mechanical strain to obtain the total effective strain [D1]. This strain becomes the starting point for a calculation of the crack-driving force. In some procedures, residual strains, being self-equilibrating, are treated differently from mechanical strains [D2]. These analytical treatments have been justified on the basis of experimental evidence of the adverse effect of residual stresses on fracture loads, failure analyses that list residual stresses as a contributing cause of failure, and engineering judgment.

However, few straightforward calculations of the effect of residual stresses on crack-driving forces are available. The state of the art is indicated by a recently published finite-element analysis of a center-cracked tensile panel subjected to thermal and mechanical loading [D3]. Therefore, the opportunity exists to utilize experimentally derived information on the effect of residual stresses on fracture driving forces to verify and improve FFS assessment methods and to provide information for specific cases not covered by these methods.

This paper reports the first use known to the author of the technique of measuring contour strains to evaluate the applied J-integral produced by residual stresses in simulated repair welds.

The technique of direct measurement of the J-integral has been applied to base-metal plates in tension and bending for various crack sizes and up

to applied strain levels well beyond yield [D4,D5]. The uncertainty of the results was estimated at 10 percent in one base-metal study [D4]. The presence of boundaries between weld metal and base metal in the specimen interior considerably complicates the conceptual basis of the measurement procedure [D6] and requires an approximation in the present technique.

MATERIALS AND SPECIMENS

Steel plate made to ASTM specification A-387 Grade 22 was used as base plate. This is a 2½Cr-1Mo pressure-vessel steel in the annealed condition. The plate thickness was 5 cm (2 in). Troughs 20 cm (8 in) long by 5 cm (2 in) wide by 3.2 cm (1-3/8 in) deep were filled with E-9018-B3L electrodes 2.3 mm (3/32 in) in diameter by the shielded-metal-arc (SMA) procedure. The yield and tensile strengths of the as-deposited weld metal were 767 and 843 MPa (111 and 122 ksi), and the base-plate yield and ultimate strengths were 270 and 499 MPa (39.2 and 72.4 ksi). Of four plate specimens tested, two were tested as-welded (AW) and two matching specimens were tested after PWHT. In the PWHT condition, the yield and ultimate strengths were 454 and 579 MPa (65.8 and 84.0 ksi). The weld properties were obtained from triplicate tensile specimens oriented along the weld direction extracted from duplicate welds. The base-metal properties were supplied by the steel maker.

The J-integral measurements were made in simulated repair welds in large plates 70 cm (27 in) wide by 180 cm (72 in) long. Two weld geometries were used: a simple trough and a simulated boiler tube-hole-ligament repair; these are shown in figure D1. The simple troughs were 20 cm × 5 cm × 3.2 cm (8 in × 2 in × 1-3/8 in), as described above. The notch was cut perpendicular to the weld direction, starting at the surface and cutting toward the back face with a circular saw 7.0 cm (2-3/4 in) in diameter. This diameter imposed a relation between cut depth and cut length such that at a depth of 3 mm (1/8 in), the length was 28 mm (1-1/8 in); at a depth of 6 mm (1/4 in), the length was 39 mm (1-1/2 in); and at a depth of 10 mm (3/8 in), the length was 49 mm (1-15/16 in).

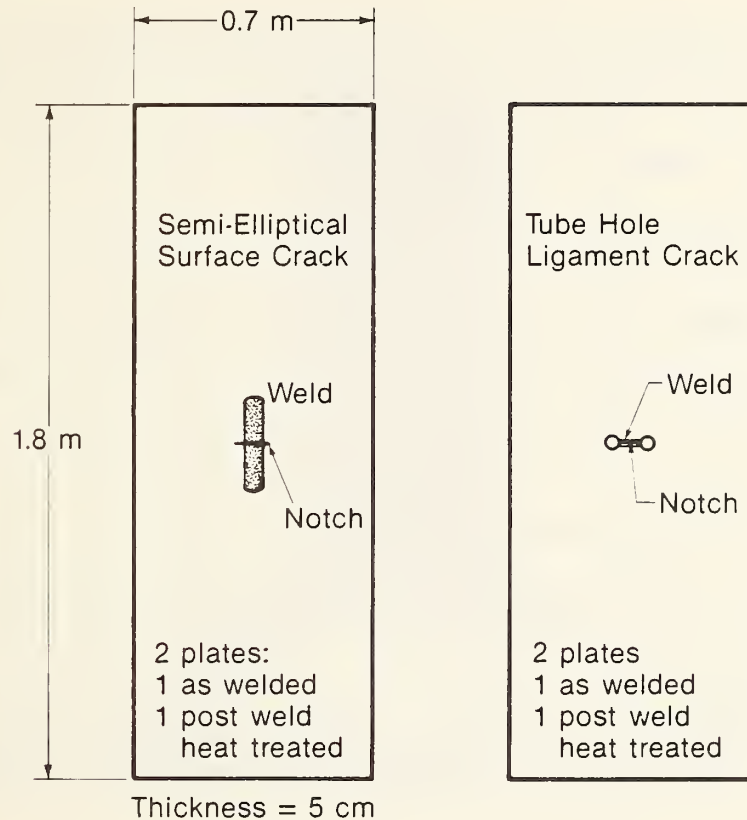


Figure D1. Weldments of the wide-plate 2½Cr-1Mo steel used in this study.

The two simulated tube holes were 3.2 cm (1-1/4 in) in diameter, separated by a ligament of width 2 cm (3/4 in). In the ligaments, a deep groove was machined extending from one hole to the other; it was filled with weld metal. The machined notch extended from one hole to the other, starting at the front surface and penetrating into the ligament thickness.

TECHNIQUE AND INSTRUMENTATION

Strain gages were located on a contour extending along the weld both on the front face where the notch opened and on the back face (opposite). In the first specimen 34 gages were used, but in the others only 8 or 9 gages were needed. The strain-gage layouts are shown in figures D2 and D3. After

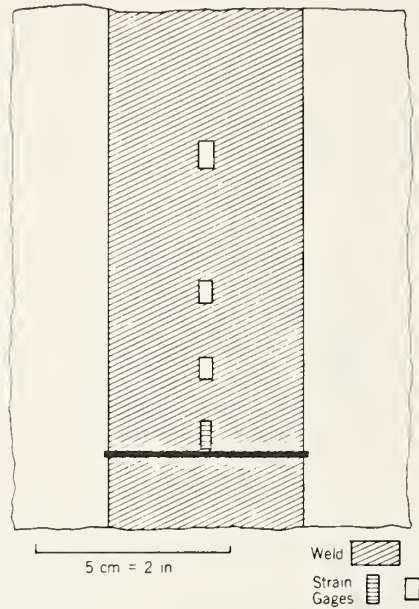


Figure D2. Strain-gage layout on the front side of the plate for measurement of the applied J-integral in a trough weld.

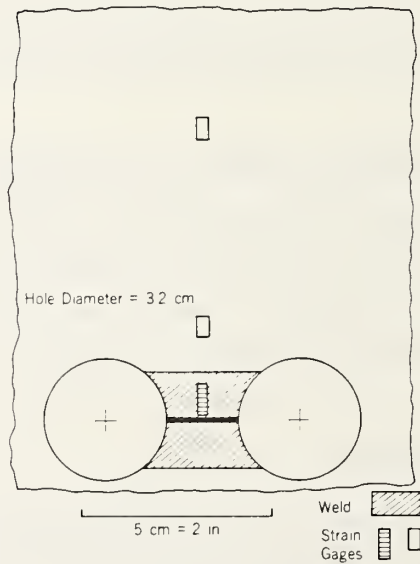


Figure D3. Strain-gage layout on the front side of the plate for measurement of the applied J-integral in a tube-hole ligament.

the first test showed that the relaxations on the back face were minimal, only one gage was used on the back face; it was positioned directly opposite the notch location. A beam instrumented with an LVDT was used to indicate the overall relaxation of the plate during the cutting.

The strain gages were wired to a microcomputer-based amplification and recording system that provided a reproducibility of about 5×10^{-6} strain for all except one gage, which was excluded from the analysis because of drift. Near the cut, an array of small gages separated by 1.5 mm was used. The center of the gage closest to the mouth of the cut was about 2 mm from the cut. The width of the saw blade was 1.5 mm.

After setup, checkout, equilibration, and recording of the zero point data, the procedure was to lower the circular saw blade into the cut until the depth was increased by about 1 mm (0.04 in), then to stop cutting to measure the new cut depth and to record the strain gage strains and the plate deflection indicator reading. The test itself required approximately a half day for a final cut depth of about 14 mm (1/2 in).

ANALYSIS

Measured Strain Relaxations and Residual Strains

The measured strain relaxations of the front face gages were compressive, indicating the relaxation of a state of residual tension. The relaxation strains decreased with distance from the cut, as required by St. Venant's principle. In the PWHT plates, the straight-line dependence of the strain relaxation on the distance from the cut in a semilog plot (figs. D4 and D5) indicated an exponential decay. The strains were extrapolated to the cut location. Converting to stress using the elastic modulus gave residual stresses of 325 MPa (47.1 ksi) at the semielliptical surface crack and 55 MPa (8.0 ksi) at the tube-hole-ligament crack. Transverse gages, not shown in figures D2 and D3, relaxed only slightly, so that no contribution from transverse strains was used in the residual stress calculation.

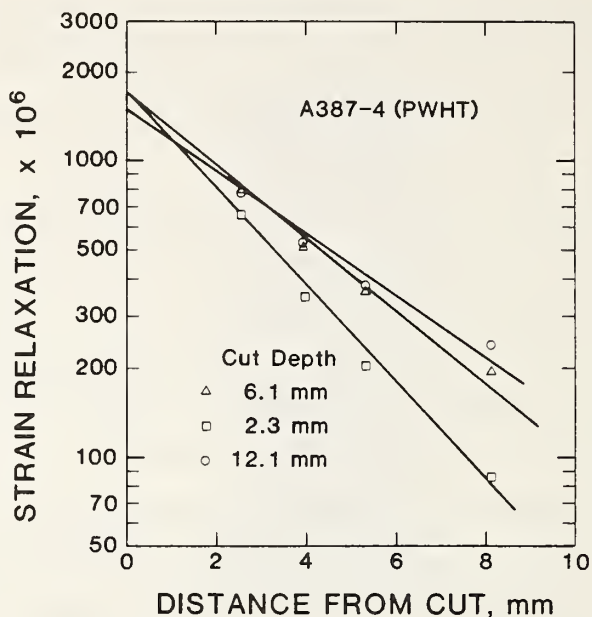


Figure D4. Strain relaxation versus distance from cut in a PWHT trough weld. Cut length increases along with the depth, as noted in the text.

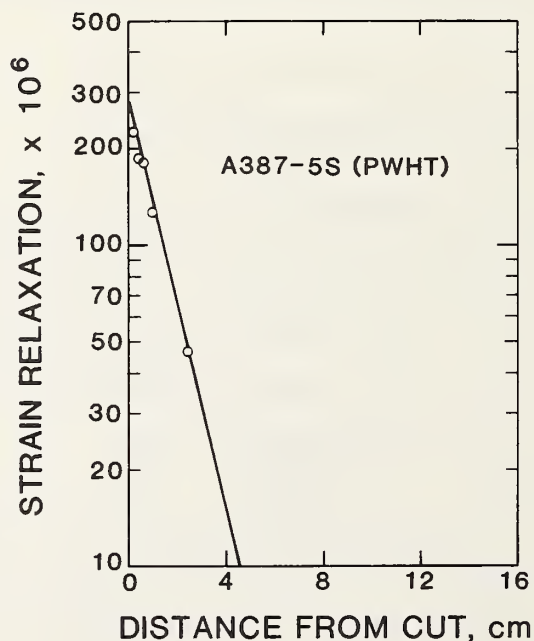


Figure D5. Strain relaxation versus distance from cut in a PWHT simulated tube-hole ligament weld.

In the AW plates, the dependence of the strain relaxation on the distance from the cut was more difficult to understand (figs. D6 through D8). Far from the cut, the dependence was exponential, as before; but near the cut, a saturation occurred, so that the measured strains were below the extrapolated value. Figure D7 illustrates this behavior in detail. The saturation strain level is roughly equal to the base-metal yield strain.

For the J-integral calculations, a value of the residual strain was needed. For the PWHT plates, the extrapolated value at the cut location seemed appropriate. However, for the AW plates, because the measured strain relaxations near the cut were below the extrapolated value, the strain value at saturation was used.

These observations seem to indicate that the severity of a residual stress field depends not only on its peak magnitude but also on its spatial distribution.

Crack-mouth-opening displacement (CMOD) was obtained by integrating the measured strains. The total y-direction displacement over the instrumented contour was assumed to be zero, because of the restraint provided by the large specimen plate. So

$$\int_0^L \epsilon_{yy} dy + \frac{1}{2} \text{CMOD} = 0, \quad (\text{D1})$$

using the assumption of symmetry. CMOD was obtained by using equation D1.

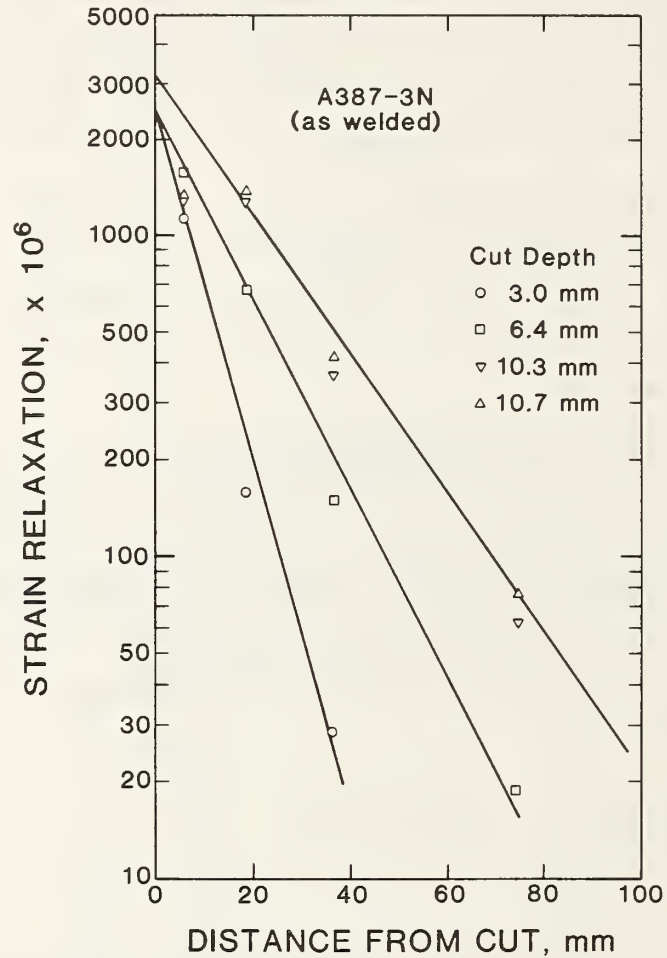


Figure D6. Strain relaxation versus distance from cut in an AW trough weld. The cut length increases along with the depth, as noted in the text. Each of the symbols at 4 mm from the cut represents an approximate average, excluding outliers, of the maximum strains from an array of small gages near the cut. The actual data from these are shown in figure D7.

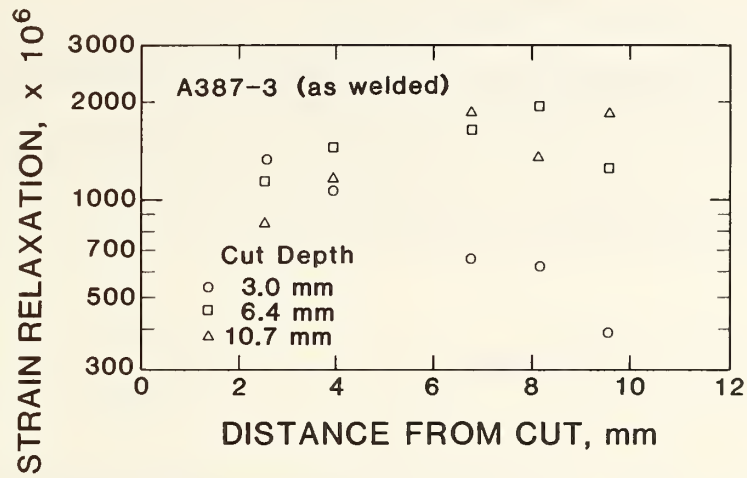


Figure D7. Strain relaxation near the cut in an AW trough weld.

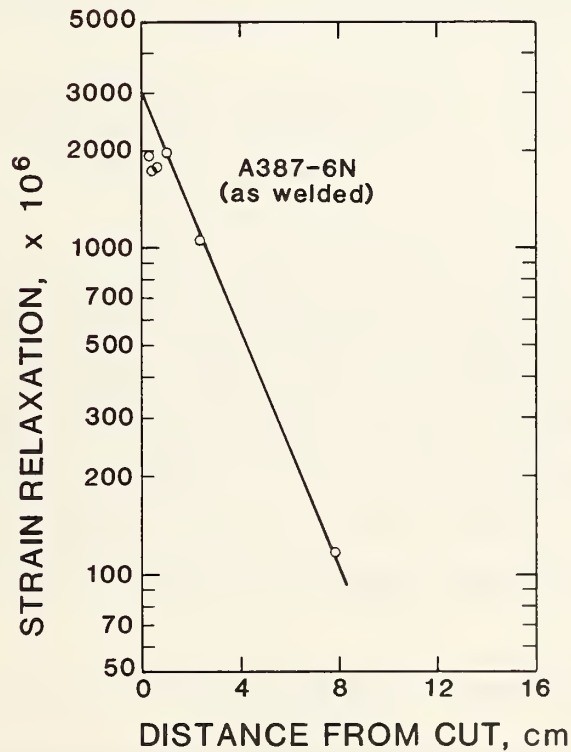


Figure D8. Strain relaxation versus distance from cut in an AW simulated tube-hole-ligament weld.

Accounting for the Weld in Calculating the J-Integral

Although an expression for the J-integral that includes thermal stresses and strains has been derived [D7], it seemed preferable here to treat the weld as a bimaterial composite of base metal and weld metal. Within each, the J-integral is path-independent, as usual. The definition is

$$J = \int_{\Gamma} W dy - \vec{T} \cdot \vec{u}/dx ds \quad (D2)$$

where, as usual, x and y are Cartesian spatial coordinates with their origin at the crack mouth, with x the direction of self-similar crack propagation and y the direction perpendicular to the crack plane; Γ is a contour enclosing the crack tip, W is strain work density, \vec{T} is traction normal to the contour, \vec{u} is displacement, and ds is increment of arc length along the contour. Usually, the combination of strain measurements on half of the contour (say, $y > 0$ only), the measured CMOD, and the assumption of symmetry about the crack plane enable both terms of equation D1 to be evaluated, with some cancellation of errors between the two terms.

However, because of the yield strength mismatch between the present specimen base and weld metal, the J-integral is not path-independent for contours that lie partially in the base metal and partially in the weld metal. In the present case, the experimental contour cannot be restricted to the weld metal, because the weld is in a groove. Therefore, an additional term in the J-integral relating to the interface between the weld metal and the base metal must be considered. Mathematically,

$$J = J_{\text{usual}} + J_{\text{interface}} \quad (D3)$$

The second term in equation D2, the traction-bending term, could not be measured in the present case because the CMOD was not measurable directly. Equation D1 implies that this term is zero. The contour was chosen so that

the end lay as far as possible from the crack plane, and thus the traction-bending term would be small. The severe restraint provided by the large-plate specimen contributes to minimizing the traction-bending term. The assumption is:

$$J_{\text{usual}} = -J_{\text{front face}} + J_{\text{back face}} \quad (\text{traction-bending neglected}) \quad (\text{D4})$$

where

$$J_{\text{front face}} \equiv \int_0^L W \, dy, \quad (\text{D5})$$

front face

and $J_{\text{back face}}$ is defined similarly.

In strain-gage measurements of the J-integral in base metal with no crack ($a = 0$), the magnitudes of the front-face and back-face terms would both increase with strain, but they would cancel each other. That is,

$$J = -J_{\text{front face}(a=0)} + J_{\text{back face}(a=0)} = 0 \quad (\text{base plate}) \quad (\text{D6})$$

where a is crack depth.

After the notch is cut, the strains near the crack mouth relax, causing W to decrease and thus reducing the magnitude of the front-face term and increasing the total J-value. Under normal conditions, that is, when the crack depth is less than half the plate thickness and when there is no net section yielding, the back-face term remains about the same as it would have been if there were no crack. Therefore, for a given strain level,

$$J_{\text{back face}(a)} \approx |J_{\text{front face}(a=0)}| \quad (\text{normal conditions}) \quad (\text{D7})$$

and

$$J \approx -|J_{\text{front face}(a)}| + |J_{\text{front face}(a=0)}| \quad (\text{normal conditions}) \quad (\text{D8})$$

where the absolute value signs have their usual meaning.

In a weldment, equations D3 and D4 become

$$J = -J_{\text{front face}} + J_{\text{back face}} + J_{\text{interface}} \quad (\text{D9})$$

The difficulty in evaluating J in equation D9 is the interface term. Equation D9 must apply both before and during the cutting of the notch. Before cutting, the full residual strains are present, but the total J-integral must be zero, because, as yet, there is no notch:

$$J = 0 = -J_{\text{front face}}(a=0) + J_{\text{back face}}(a=0) + J_{\text{interface}}(a=0) \quad (\text{D10})$$

where a is crack length.

Therefore, an expression for J can be formed from equations D9 and D10:

$$J = -J_{\text{front face}}(a) + J_{\text{back face}}(a) + J_{\text{interface}}(a) \quad (\text{D11}) \\ + J_{\text{front face}}(a=0) - J_{\text{back face}}(a=0) - J_{\text{interface}}(a=0)$$

Equation D11 shows that what is needed is the change in the interface term, rather than in its absolute value. This term cannot be measured experimentally because the interface is buried within the specimen. Therefore, the behavior of the interface term can only be assumed. The known behavior of the back-face strain relaxations provides a clue. These relaxations were measured and found to be small; the interface is much closer to the back face than to the front face, so the strain relaxations at the interface should also be small. Therefore, the interface term of the J-integral was assumed to remain constant during cutting. That is,

$$J_{\text{interface}}(a) = \text{constant} \quad (\text{assumption}) \quad (\text{D12a})$$

$$J_{\text{interface}}(a) - J_{\text{interface}}(a=0) = 0 \quad (\text{D12b})$$

Various arguments in support of equation D12 were considered, but none seemed definitive. Therefore, equation D12 is treated here as a needed and plausible assumption.

From equations D11 and D12,

$$J = -J_{\text{front face}}(a) + J_{\text{front face}}(a=0) \quad (\text{D13}) \\ + J_{\text{back face}}(a) - J_{\text{back face}}(a=0)$$

Because the changes in $J_{\text{back face}}$ during cutting were small, equation

D13 for welds is essentially the same as equation D8 for base plate. Equation D13 was used to estimate the applied J-integral in the present weld specimen experimentally. The uncertainty results from the assumptions in equations D4 and D12. The uncertainty in the J-integral was estimated to be plus or minus 20 percent.

RESULTS AND DISCUSSION

The measured J-integral values are plotted against crack depth in figure D9. The clear differences between the AW and PWHT plates result from the higher residual strains in the AW plates. The initial linear increase of J-integral with depth and the saturation at the latter stages are as anticipated from results reported in the literature for semielliptical surface flaws in tension and bending.

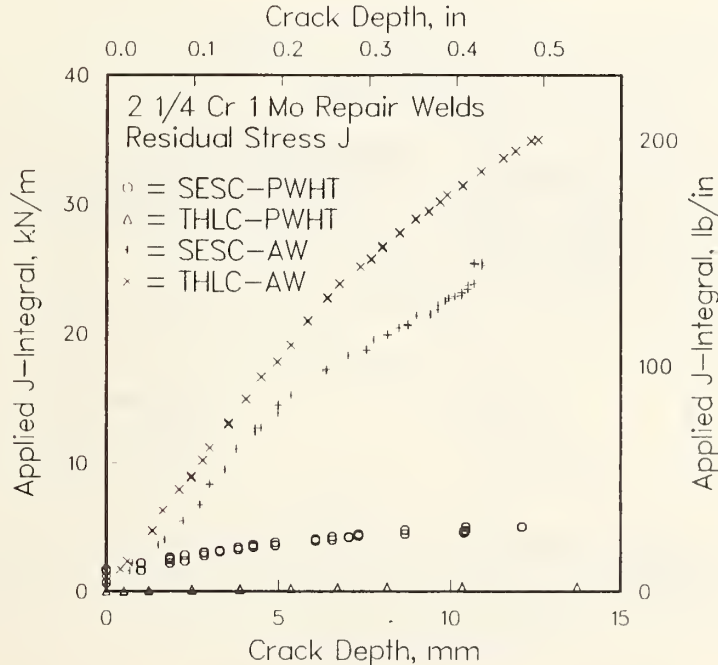


Figure D9. Measured applied J-integral values plotted against cut depth. SESC = surface crack in trough weld THLC = surface crack in tube-hole-ligament repair weld

Stress intensity, K , values for a surface-cracked plate in bending, calculated by Newman and Raju [D8], were converted to units of J-integral using the standard formula $K = (E \cdot J)^{1/2}$, where E is Young's modulus, for comparison to the present results (fig. D10). The approximate agreement of the present results with the Newman-Raju values was obtained by choosing a stress level of 519 MPa (75.2 ksi), which is equal to the average of the yield strengths of the weld and base metal. This stress is higher than the measured residual stress of 372 MPa (54 ksi). The extrapolated residual strain at the cut location was 2.6×10^{-3} . When converted to stress this gives 538 MPa (78 ksi), which would also give approximate agreement between predicted and measured applied J-values. The agreement between the present results and the Newman-Raju results supports the validity of the present results.

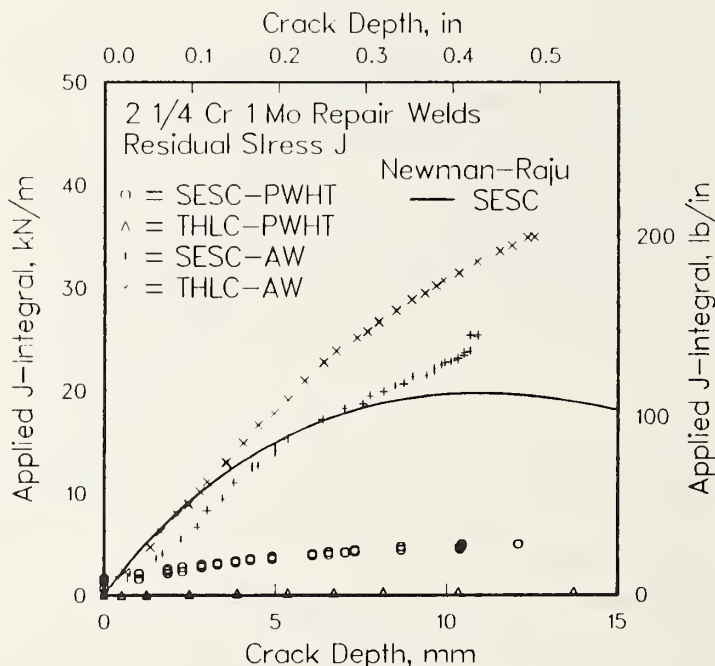


Figure D10. Comparison of calculated and measured J-integral values as a function of cut depth.

The calculation of CMOD from measured strains is straightforward. Therefore, it would be attractive to correlate measured CTOD and J-integral with calculated CTOD and J-integral to verify the measured J-values. But only approximate calculated CMOD values are available for surface cracks in tension [D9] and none are available for surface cracks in bending. Therefore, ratios of K to CMOD from calculations for single-edge cracks in tension and bending and for surface cracks in tension were compared with the experimental ratio of K to CMOD. The ratios are listed in table 1 for the final crack depth of the surface-cracked specimen. These data indicate that the present results for the ratio of K to CMOD are consistent with the trend of the calculated values for single-edge cracks. The handbook ratio for bending is about 10 percent less than for tension; the present value for a semielliptical surface crack is about 10 percent less than that for such a crack in tension.

Table 1. Normalized ratio of K to CMOD, $\frac{K}{E \cdot \text{CMOD}}$, for various crack types at $a = 10.9 \text{ mm (0.428 in)}$.

Type	$K/(E \cdot \text{CMOD}), \text{ cm}^{-\frac{1}{2}}$	$K/(E \cdot \text{CMOD}), \text{ in}^{-\frac{1}{2}}$
Center crack, tension	0.425	(0.677)
Single-edge crack, tension	0.324	(0.516)
Single-edge crack, bending	0.283	(0.451)
Semielliptical surface crack, tension	0.379	(0.604)
Present, semielliptical surface crack	0.338	(0.539)

SUMMARY

A destructive technique has been demonstrated for measurement of the applied J-integral produced by residual strains from welding. This technique clearly distinguishes as-welded from stress-relieved plates. The applied J-integral was much higher in two AW plates than in two postweld heat treated plates. The technique shows the increase of J-integral with crack depth. The measured J-values, converted to units of stress intensity, approximately matched those calculated for a yield-level bending stress applied to an equivalent plate, when the effective yield stress was taken as the average of base-metal and weld-metal yield stresses. The J-values for a crack in a simulated boiler tube-hole-ligament repair were slightly lower than those for a semielliptical surface crack in a repair weld in an intact plate.

ACKNOWLEDGMENTS

The financial support provided by the Naval Sea Systems Command through its project sponsor Commander L. R. Easterling is gratefully acknowledged. Helpful discussions with W. C. Fraser and M. A. E. Natishan of the David Taylor Naval Ship Research and Development Center are appreciated. Technical assistance by J. D. McColskey, M. Moyer, and J. J. Broz of the National Bureau of Standards is also appreciated.

REFERENCES

- [D1] British Standards Institution. Guidance on some methods for the derivation of acceptance levels for defects in fusion welded joints. PD 6493: 1980, British Standards Institution, London, 1980.
- [D2] Harrison, R.P., Loosemore, K., Milne, I., and Dowling, A.R. Assessment of the integrity of structures containing defects, R/H/R6-Rev. 2. Central Electricity Generating Board, London, 1980.

- [D3] Hellen, T.K. and Blackburn, W.S. Post-yield fracture mechanics analysis of the combined thermal and mechanical loading of a centre-cracked plate. *International Journal of Fracture* 32, 1987, pp. 185-199.
- [D4] Read, D.T. Experimental method for direct evaluation of the J-contour integral, in *Fracture Mechanics: Fourteenth Symposium - Volume II: Testing and Applications*. J.C. Lewis and G. Sines, Eds. ASTM STP 791, American Society for Testing and Materials, Philadelphia, 1983, pp. II-199-II-213.
- [D5] Dodds, R.H. and Read, D.T. Experimental and analytical estimates of the J-integral for tensile panels containing short center cracks. *Int. J. Fract.* 28, 1985, pp. 39-54.
- [D6] Read, D.T. Experimental results for fitness-for-service assessment of HY130 weldments. NBSIR 84-1699, National Bureau of Standards, Boulder, Colorado, March 1984, 90 pp.
- [D7] Chell, G.G. Elastic-plastic fracture mechanics, in *Developments in Fracture Mechanics - I*. G.G. Chell, Ed. Applied Science Publishers, London, 1979, p. 97.
- [D8] Newman, J.C., Jr. and Raju, I.S. Analyses of surface cracks in finite plates under tension or bending loads. NASA Technical Paper 1578, National Aeronautics and Space Administration, October 1979, 43 pp.
- [D9] Mattheck, C., Morawietz, P., and Munz, D. Stress intensity factor at the surface and at the deepest point of a semielliptical surface crack in plates under stress gradients. *Int. J. Fract.* 23, 1983, pp. 201-212.

U.S. DEPT. OF COMM. BIBLIOGRAPHIC DATA SHEET <i>(See instructions)</i>	1. PUBLICATION OR REPORT NO. NBSIR 87-3075	2. Performing Organ. Report No.	3. Publication Date August 1988
4. TITLE AND SUBTITLE <p style="text-align: center;">POSTWELD HEAT TREATMENT CRITERIA FOR REPAIR WELDS in 2-1/4Cr-1Mo SUPERHEATER HEADERS AN EXPERIMENTAL STUDY</p>			
5. AUTHOR(S) <p style="text-align: center;">D.T. Read and H.I. McHenry</p>			
6. PERFORMING ORGANIZATION <i>(If joint or other than NBS, see instructions)</i> NATIONAL BUREAU OF STANDARDS DEPARTMENT OF COMMERCE WASHINGTON, D.C. 20234		7. Contract/Grant No. 8. Type of Report & Period Covered	
9. SPONSORING ORGANIZATION NAME AND COMPLETE ADDRESS <i>(Street, City, State, ZIP)</i> <p style="text-align: center;">Department of the Navy Naval Sea Systems Command Washington, DC 20362</p>			
10. SUPPLEMENTARY NOTES <input type="checkbox"/> Document describes a computer program; SF-185, FIPS Software Summary, is attached.			
11. ABSTRACT <i>(A 200-word or less factual summary of most significant information. If document includes a significant bibliography or literature survey, mention it here)</i> <p>Wide-plate and standard-size specimens cut from repair welds in 2-1/4Cr-1Mo plate were tested as-welded and after post-weld heat treatment (PWHT). Wide plates were prepared with surface cracks and tube-hole-ligament cracks in simulated repair welds made with the shielded-metal-arc process. The plates were instrumented with strain and displacement gages for direct measurement of the applied J-integral. After notching and fatigue precracking, the plates were tested in bending. Pop-ins occurred in the as-welded plates, but not in the PWHT plates.</p> <p>Three-point-bend specimens with cracks oriented in the TS direction were used to measure weld-metal and heat-affected-zone (HAZ) toughness values. Results of direct measurements of the applied J-integral on the wide plates were compared with critical J-value measurements of three-point-bend specimens. The comparison indicated that PWHT was highly beneficial, because it reduced the crack-driving force from residual stresses and increased the weld-metal and HAZ toughness. In the as-welded condition, very low toughness values were measured at the HAZ. These low toughness values, together with the measured crack-driving forces, indicated critical crack depths of a few millimeters.</p> <p>To extend the usefulness of these results, a new approach to the problem of the applied J-integral produced by residual stresses is being explored: strain-gage measurements made during notching are analyzed to obtain an applied J-integral as a function of crack depth. The preliminary results are encouraging. The residual-stress-produced J-value is roughly equivalent to that produced by a remote elastic loading to the same stress level.</p>			
12. KEY WORDS <i>(Six to twelve entries; alphabetical order; capitalize only proper names; and separate key words by semicolons)</i> fracture; hydrotest; J-integral; pressure vessel; residual stress; safety; stress relief			
13. AVAILABILITY <input checked="" type="checkbox"/> Unlimited <input type="checkbox"/> For Official Distribution. Do Not Release to NTIS <input type="checkbox"/> Order From Superintendent of Documents, U.S. Government Printing Office, Washington, D.C. 20402. <input checked="" type="checkbox"/> Order From National Technical Information Service (NTIS), Springfield, VA. 22161		14. NO. OF PRINTED PAGES <p style="text-align: center;">60</p> 15. Price	

